DEVELOPMENTAL AND FUNCTIONAL ANALYSIS OF SCUTES IN THE ARMORED CATFISH *CORYDORAS AENEUS*

By
Emily Volk
Ecology and Evolutionary Biology (EBIO), University of Colorado at Boulder

Defense: April 4, 2019

Thesis Advisor:
Dr. David Stock, EBIO

Defense Committee:
Dr. David Stock, EBIO
Dr. Barbara Demmig-Adams, EBIO & Honors Council Representative
Dr. Franck Vernerey, Mechanical Engineering

Acknowledgements

Thank you so much to the vast support network I have had at the University of Colorado, Boulder that made this research possible. First and foremost, I would like to send my deepest thanks to my Honors Council representative, Dr. Barbara Demmig-Adams, for becoming a key advocate and lending your immense editorial strength to making my thesis a great and approachable project to be proud of.

To Dr. David Stock, I want to extend pure gratitude for providing so many opportunities to me. Your in-depth and incredibly well-taught Fish Biology class started me on the path of wanting to gain biological expertise, which you showcase gracefully, and I so thank you for the time, attention, and generosity you have dedicated to allowing me to work in your lab with real fish specimens.

Dr. Franck Vernerey, thank you so much for providing continual inspiration, lighting-fast direction toward proper analysis and qualification, and persistent innovation in how research targets can be most relevant, cutting-edge, and creatively documented. Working with your Soft Matter Mechanics Lab has truly been a dream come true, and, as I told Tong and Shankar on my first interview, the research I now get to work on is directly what inspired me to come to university to pursue study of this continually-intriguing intersection of biology and mechanics.

An additional key thank you goes to Dr. Violet Mwaffo. Dr. Mwaffo, thank you for advising me during an instrumental turning point in my research, and guiding me with your expertise toward the proper analysis techniques for live, larval specimen research. Your help was invaluable, and I so appreciate you opening your door to my questions.

Thank you to Sharon Anderson and the Discovery Learning Apprenticeship (DLA) program for enabling me to find literally my dream research position with the Vernerey Group

Soft Matter Mechanics Lab for the 2017-18 school year, and for generously funding my research over this time.

Thank you to all members of the Soft Matter Mechanics Lab. Thank you to Zachary White for getting me started on this fish scales research through letting me assist with your master's thesis, and for being a driven role model in powering through your own thesis. Thank you to Shankar Lalitha Sridhar for calmly accepting and dissipating my panic during some of the more stressful unknowns of my research, and for your assistance with specific mechanical analyses (and wrestling MATLAB syntax into place). Thank you to Shankar and Rob Wagner for talking through different mechanical testing options, and quickly redirecting my project in even short overlaps at the Celestial Seasonings coffee bar. Tong Shen and Revathi Priyanka Mohan, even though I haven't worked with either of you directly on this project, thank you for being consistently happy, ever-helpful and welcoming research peers from the very beginning of my exposure to the Soft Matter Mechanics Lab.

Special appreciation goes out to Timothy O'Neil and the Undergraduate Research Opportunities Program (UROP). Tim, you not only were my first touch-point and welcoming presence for the Norlin Scholars cohort, but also supported innovative takes on my research in my senior year with UROP funding, which allowed me to continue to continue to work between labs in what was a vital interdisciplinary opportunity.

Thank you to Jake Lowenstein for not only teaching me how to fly fish in Boulder Creek, but for being one of my most fierce advocates in college. Thank you for your efforts in promoting and supporting my research, as well as for being a key lab educator in my time in Ecology and Evolutionary Biology.

Additionally, thank you to some of my ATLAS family. To Marisa Reynolds, thank you so much for letting me hop in and out of the College of Engineering as I pieced together my academic path. Thank you to Arielle Hein for encouraging me to merge my research and creative interests in a final physical computing project. Overall, thank you to ATLAS for being a key, interdisciplinary driver of my college experience, and for continually promoting unique and cutting-edge intersections of science and art.

Last but not least, I would like to thank my family support and academic peers, who, with equally tired but sparked looks in their eyes, were key ballasts for my research drive. Thank you for showcasing intense motivation across your individual interests, telling me it was okay not to go rock climbing while I pursued my personal goals, and supporting this project with feedback, encouragement, and shared work days.

My pride in this thesis is amplified by being able to share it with you. Thank you, all, for your critical roles in my undergraduate research experience.

TABLE OF CONTENTS

Abstract

Fish scales are specialized biological structures of current interest in innovative materials design because of the combination of protective function, flexibility, and light weight they offer. This study presents a developmental and functional investigation of a particular fish scale structure, the scutes (bony external plates) of the armored Bronze Corydoras Catfish (*Corydoras aeneus*). Scutes in this model fish species were analyzed via three complementary approaches. First, scutes were documented throughout fish development via high-quality microscope images. These images were subsequently used to inform fabrication of synthetic models to characterize the relationship between scute overlap and overall bending stiffness of scute assemblies. These models indicated that scute overlap resulted in a 318% increase in bending stiffness. My study also presents insight into how increased bending stiffness could influence the swimming strategy of live larval *C. aeneus*. By synthesizing the insight from these developmental and functional investigations of the scutes of *C. aeneus*, my study aims to contribute to a better functional understanding of the evolutionary pathway of *C. aeneus* as well as inform fabrication of future innovative designs utilizing the unique structure and dynamics of scute assemblies.

Introduction

Biological structures and systems are tuned through evolution for particular environments and functions. The study of biological (natural) features can offer illuminating insight into uniquely optimized systems. Scales are surface features widely exhibited across species and environments (White and Vernerey 2018). The scaled skins of fishes are of current interest in innovative materials design. Due to their unique structure and morphology, fish scales offer a combination of high protection, light weight, and flexibility. Specifically, the integumentary (skin) systems of many fishes combine the protective benefit of assemblies of tough scales made of hard, biomineral components with the flexibility of underlying soft tissue to achieve unique combinations of protection and mobility (Marino Cugno Garrano et al. 2012; Zhu et al. 2013; Browning et al. 2013; Vernerey et al. 2014; Vernerey and Barthelat 2014). Various fish scale structures have evolved within fishes, and exhibit a diversity of shapes, sizes, compositions, and arrangements (Ibañez et al. 2016; White and Vernerey 2018). Although scale morphology has been widely characterized across species for use in taxonomic identification (classification) of species (Jawad et al. 2005; Ibañez et al. 2009; Bräger et al. 2017), the structure and mechanics of fish scale assemblies are a more recent subject of research. Investigating the mechanical actions of fish scale assemblies is of current interest (Marino Cugno Garrano et al. 2012; Zhu et al. 2013; Browning et al. 2013; Ghosh et al. 2014; Vernerey et al. 2014; Vernerey and Barthelat 2014; Funk et al. 2015; Vernerey and White 2018) to improve understanding of potential functions of these unique surface features in nature, as well as to apply the findings to innovative, human-centered designs.

The characteristics of fish scale assemblies relevant to innovative materials design include remarkable toughness and puncture resistance, which serves a protective function while remaining lightweight (Chen et al. 2011; Marino Cugno Garrano et al. 2012; Zhu et al. 2012; 2013; Browning et al. 2013). Fabrication of synthetic analogues of fish scale assemblies for flexible, lightweight protective armors has been a recent research target (Zhu et al. 2013; Chintapalli et al. 2014; Funk et al. 2015; Torres et al. 2015). An additional goal is understanding how the mechanical dynamics of overlapping fish scale assemblies may relate to efficient locomotion (swimming strategy). As overlapping fish scales interact during movement, scaled skins exhibit “strain-stiffening response,” an increase in bending stiffness as curvature of bending increases (Vernerey and Barthelat 2010; Rudykh and Boyce 2014; Vernerey et al. 2014). Bending stiffness has been hypothesized to play a key role in energy restitution (Vernerey et al. 2014; Szewciw and Barthelat 2017; Szewciw et al. 2017) and swimming strategy (Wainwright 1978; Hebrank 1980; Hebrank and Hebrank 1986; Long et al. 1996; Tytell et al. 2010) across scaled fish species, and has also been tuned to optimize the performance of biomimetic structures such as swimming robots (Long et al. 2006; Cui and Jiang 2016; Jusufi et al. 2017) and hydrodynamic foils modeled on simplified body shapes of fishes (Lauder et al. 2011; 2012; Shelton et al. 2014; Feilich and Lauder 2015; Lucas et al. 2015). To better understand the function of bending stiffness of fish scale assemblies, an emerging research question is the possible function of fish skin in efficient locomotion during swimming. Determining the functions of scales in movement is critical to understanding the properties of efficient locomotion techniques of both natural and biomimetic structures.

My study focused on scutes as a particular type of fish scale. Scutes are bony plates that form through ossification (the hardening of soft tissue into bonelike material) of cells in the inner (dermal) layer of the skin. Scutes exhibit notable density and toughness in contrast to more flexible (elasmoid) scales (Ebenstein et al. 2015). While the trend in the evolution of scales in most fishes has been from away from thick armor plates to reduced, more flexible scale assemblies, several lineages of fishes have re-evolved armor in the form of scutes (Harder 1976; Whitear 1986; Sire 1993; Elliot 2000; Sire et al. 2009; Schultze 2016; 2018). Previously characterized aspects of scute morphology include their shape (Sire and Huysseune 1996), density (Ebenstein et al. 2015) and surface morphology (Sire and Huysseune 1996; Rivera-Rivera and Montoya-Burgos 2017). However, the particular mechanics of overlapping scute assemblies have yet to be investigated.

My study focuses on developmental and functional aspects of the scutes of the Bronze Corydoras Catfish (*Corydoras aeneus*). Specifically, I investigate the functional consequences of scute overlap in this model species. *C. aeneus* is a member of the family Callichthyidae, in which scutes and their arrangement are highly conserved features. Insight into the function of particular scute assemblies of *C. aeneus* could thus be extended to other species in this family. Scutes in the Callichthyidae are arranged along the trunk of the fish in a dorsal (top) and ventral (bottom) row. These rows partially overlap with each other along the horizontal midline of the fish. Similarly, individual scutes also overlap within rows. Scute overlap allows for interactions between scales that may contribute to mechanical response of the overall scute assembly. It is the effect of scute overlap on stiffness and locomotion that is the subject of the present study. My study analyzed the functional consequences of overlap in scute assemblies of *C. aeneus* via three complementary approaches. First, the formation of scute assemblies during larval development was characterized via microscopy across a series of stages. The resulting images were used to inform fabrication of synthetic samples to test how scute overlap relates to overall bending stiffness of scute assemblies. These latter results were related back to live specimens through video analysis of larval locomotion at different developmental stages for an assessment of whether bending stiffness of scute assemblies may influence swimming strategy of these fish. My study thus synthesized developmental and functional assessment of the scutes of *C. aeneus*. These findings may elucidate functional understanding of the evolution of scutes in the Callichthyidae as well as improve future biomimetic designs based on these particular scale structures.

Guiding Questions

- How does scale morphology relate to the mechanics of scaled systems?
- How do the scutes in *C. aeneus* change over the course of development? At what developmental stage do scutes begin to overlap?
- Is there evidence that scute assemblies influence swimming strategy?
- Can characteristics of natural fish scales and scutes inform specific aspects of novel designs for flexible, bioinspired analogues to scaled skin?

Hypotheses

1. Scutes contribute to the mechanical response of fish skin. Specifically, overlap of scutes in *C. aeneus* is associated with greater bending stiffness.
2. If scute overlap is associated with greater bending stiffness, scute overlap will also correlate with a change in locomotive strategy in *C. aeneus*.

Background: Synthesizing current mechanical understanding of fish scale assemblies

Strain-stiffening response

An increase in material stiffness when bent, curved, or otherwise deformed is a response known as strain-stiffening. Strain-stiffening response is a characteristic shared by a large number of biological structures and materials to redistribute stress throughout a structure (Erk et al. 2010). Fish scale assemblies exhibit characteristic strain-stiffening response under curvature (Vernerey and Barthelat 2010; Rudykh and Boyce 2014; Vernerey et al. 2014). The overlap of fish scales serves to increase the mechanical resistance of the skin as it is deformed, as studied in natural (Zhu et al. 2013), synthetic (Ghosh et al. 2014; Funk et al. 2015), and mathematical models (Vernerey et al. 2014). Such "flexural resistance" to bending is a key focus area in the mechanical study of fish skins (Vernerey and Barthelat 2010; Zhu et al. 2013; Rudykh and Boyce 2014; Vernerey et al. 2014; Ghosh et al. 2014; Funk et al. 2015).

Flexural resistance and strain-stiffening response of fish scale assemblies depend on various factors, including scale composition, shape, thickness, degree of overlap (termed "imbrication"), and proportion of total area embedded in the dermal pocket (Vernerey and Barthelat 2010; Vernerey and Barthelat 2014). Fishes exhibit a wide variety of scale morphologies (Ibañez et al. 2016; White and Vernerey 2018), and species-specific scale morphology must be considered to accurately characterize the mechanics of unique fish scale structures. My study investigates the response of the particular morphology of the overlapping scutes of *C. aeneus*.

Protection

As stated above, the strain-stiffening response of fish scale assemblies is of interest in the context of protection with application to lightweight, flexible armor designs (Zhu et al. 2013; Chintapalli et al. 2014; Funk et al. 2015; Torres et al. 2015; White and Vernerey 2018). Since a threat to a fish, such as a bite from a predator, most likely impacts an area involving more than one scale, overlapping scales are beneficial by virtue of spreading the force of a puncture threat across an assembly of scales, which dissipates the delivered energy across a larger area

(Vernerey and Barthelat 2010; Zhu et al. 2013; Vernerey and Barthelat 2014) and lessens damage to soft tissue directly underneath a puncture threat.

Another key feature in the protective capacity of fish scales is the puncture resistance of individual scales, which can protect against sharp threats such as bites incurred from predation. Individual fish scales are remarkably puncture resistant (Chen et al. 2011; Marino Cugno Garrano et al. 2012; Zhu et al. 2012; 2013; Browning et al. 2013). For example, the strength of a fish scale subjected to sharp indentation by a needle was beyond that of polycarbonate (Zhu et al. 2012), a strong, synthetic composite. The puncture resistance of fish scales is largely due to the material composition of individual scales. Because they are made of cellular bone overlain with an enamel-like substance (Sire et al. 2009), scutes exhibit density and strength greater than most fish scales, and function as tough armor plates.

An evolutionary perspective

Fish scales contrast with the scales of reptiles and birds in both their composition and how they form (Elliot 2000). Fish scales are mineralized structures that form in the inner (dermal) layer of the skin, whereas scales of reptiles and birds form in the outer (epidermal) layer of skin, and are made of keratin proteins, similar to hair, feathers, hoofs and claws (Elliot 2000). Scales of bony fishes can be classified into two main categories based on shape and structure: rhombus-shaped (ganoid) scales and round (elasmoid) scales (Harder 1976; Whitear 1986; Elliot 2000; Sire et al. 2009; Schultze 2016; Schultze 2018). Ganoid scales represent the ancestral condition and persist in only a few lineages of extant (surviving) fishes, namely the families Polypteridae (bichirs of Africa) and Lepisosteidae (gars of North America) (Nelson et al. 2016). Ganoid scales are thick and individually inflexible, consisting of an inner bony layer and an outer hyper-mineralized, enamel-like layer (ganoine), with (polypterids) or without (lepisosteids) an intervening layer resembling the dentine of teeth. Flexibility of the scale assembly as a whole is maintained by minimal overlap between scales, being confined to narrow peg-and-socket articulations between neighbors (Harder 1976; Grande 2010). In contrast, elasmoid scales, which are characteristic of most teleost fishes (96% of living bony fish species – Nelson et al. 2016), are thin and flexible, consisting of mineralized collagen fibers (Harder 1976; Whitear 1986; Elliot 2000; Sire et al. 2009; Schultze 2016; Schultze 2018). Greater overlap between neighboring elasmoid scales is likely to compensate for their thinness by increasing stiffness of the assembly to allow for mechanical protection (Harder 1976).

While the trend in the evolution of scales in most fishes has been from a thick "armor" to a reduced, more flexible covering, several lineages of teleost fishes have re-evolved armor in the form of bony plates known as scutes (Harder 1976; Whitear 1986; Sire 1993; Elliot 2000; Sire et al. 2009; Schultze 2016; Schultze 2018). These include members of the orders Syngnathiformes (seahorses and pipefishes), Gasterosteiformes (sticklebacks), Tetraodontiformes (puffers), and Siluriformes (catfishes). Interestingly, the scutes of the armored catfish family Callichthyidae have converged on the individual structure of the ganoid scales of gars, consisting of a thick basal layer of bone covered with an enamel-like tissue known as hyaloine (Sire 1993). These scutes are arranged on the flank in a dorsal and a ventral row that partially overlap with each other on the horizontal midline. Significantly, they also overlap along the anterior-posterior axis within rows in a manner more similar to elasmoid scales than to ganoid scales. It is the effect of this overlap on stiffness and locomotion that is the subject of the present study.

Scales and swimming

The increased flexural resistance of fish scale assemblies, while often studied in the context of puncture resistance for flexible armor systems (Zhu et al. 2013; Chintapalli et al.

2014; Funk et al. 2015; Torres et al. 2015), may also contribute to swimming (Vernerey et al. 2014; Szewciw and Barthelat 2017; Szewciw 2017). Specifically, increased bending stiffness of fish skin at high curvature that results from overlapping scale interactions may store elastic strain energy at the end of each stroke. Passive release of this energy would allow scales to act as an external tendon, or exotendon, to increase energy efficiency of swimming.

The action of fish skin in the undulatory locomotion of particular fish species has previously been investigated. Long et al. (1996) were the first to test how fish scales effect flexural stiffness and, in turn, undulatory wave propagation in Longnose Gar. Dermal cuts to the skin and subsequent removal of the caudal scale row of the Longnose Gar resulted in increased average body curvature during normal forward swimming and decreased flexural stiffness of the body when compared to an unmodified control. The removal of the caudal scale row resulted in significant difference in tail beat amplitude, wave speed, and relative total power compared to dermal cuts, showing significant contribution of fish scales in regulating undulatory locomotion.

Prior research suggests that the locomotive function of scale assemblies may depend on scale morphology, particularly scale density and stiffness. Increasing bending stiffness under curvature was observed in the Striped Bass (*Morone saxatilis*), but scales did not show significant contribution when compared with other layers of the dermis via soft tissue incision (Szeweiw and Barthelat 2017). This finding is likely due to differences in scale composition between the dense, highly-mineralized ganoid scales of Gars and lightweight, flexible elasmoid scales of most fish. Scutes, as thick, bony, mineralized scale features, are compositionally similar to the (ganoid) scales of Gars. The density and stiffness of scutes suggests that, in overlapping arrangements, scute assemblies may play a functional role in fish locomotion.

Pattern of scale development

Previously observed patterns of scale development are consistent with the hypothesis that fish scales assist with lateral undulations used in particular swimming strategies. Sire and Akimenko (2004) observed that the first scales to appear during larval development in the Zebrafish (*Danio rerio*) were located along the midline row at the level of the caudal peduncle, which is the narrowest region of a fish's body immediately prior to the tail. The caudal peduncle has been shown to be a key region driving swimming speed and strategy (Blake 2004; Esposito et al. 2012). Scales then appeared along the midline row and spread dorsally (toward the upper side) and ventrally (toward the underside) (Sire and Akimenko 2004). As a fish grows, scales also increase in size through addition of circuli (growth rings) at the scale margin (Ibañez 2008). Insight from models of scale growth (Smolyar and Bromage 2004; Szypula 2005) suggest that this pattern of scale development results in increased scale size and density in the caudal (tail) region, which may further contribute to increased strain-stiffening response in this key locomotive area (Vernerey et al. 2014). My study of patterns of scute development in *C. aeneus* builds on these previous case studies by adding functional assessment.

Fabrication of biomimetic systems

In general, natural structures and systems often exhibit unique features tuned by evolution for particular efficiency in specific environments. Innovative new designs can utilize inspiration from natural systems to fabricate efficient mechanical systems informed by understanding of particular evolutionary adaptations. Modeling synthetic, or human-made, systems based on inspiration from natural systems is known as biomimicry. Biomimetic design is becoming increasingly popular in engineering novel structures and materials. Fish, in particular, can provide rich inspiration for innovative designs. Importantly, fishes are able to swim with efficiency, speed, and maneuverability that can inform optimization of mechanical models for aquatic propulsion (Lauder et al. 2011). The applications of biomimetic designs inspired by fish, such as swimming robots, are far-reaching and include seabed exploration, under-water transportation, search and rescue, and more (Cui and Jiang 2016).

Aquatic robots have been designed in recent years to incorporate aspects of the functional design of swimming fish. Some biomimetic swimming robots are fabricated in order to tune mechanical variables in a synthetic system to better understand natural fish swimming strategies (Long et al. 2006; Cui and Jiang 2016; Jusufi et al. 2017), whereas other models seek inspiration from natural systems to optimize locomotive efficiency in simplified systems, such as hydrodynamic foils (Lauder et al. 2011; Lauder et al. 2012; Shelton et al. 2014; Feilich and Lauder 2015; Lucas et al. 2015).

Biomimetic mechanical systems based on fishes have already contributed to an increased understanding of the function of fish scales and skin in swimming efficiency. Even without full incorporation of specific factors contributing to locomotive efficiency in fish, a fin fabricated with bio-inspired stiffness profile and geometry has already managed to mimic fish locomotion (Salumäe and Kruusmaa 2011). Additionally, measurements of the swimming speeds of flexible materials that were identical except for their flexural stiffness show that there can be an optimum stiffness for which swimming speed is maximized for a given motion program (Lauder et al. 2010; 2011; Esposito et al. 2012). These studies further suggest an important locomotive function for bending stiffness in fishes that can, in part, be attributed to overlapping scales.

Materials and Methods

1. Documentation of pattern of scute development

The pattern of scutes can provide insight into the potential function(s) of these important surface features. Here, the developmental pathway of scutes along the trunk of *C. aeneus* specimens was assessed and documented using confocal microscopy (Olympus Cell Voyager CV1000 Disk Confocal Microscope) with a 10x objective. Confocal images were gathered of larval *C. aeneus* specimens at different time points throughout growth. In preparation for imaging, specimens were cleared and stained with alizarin red to highlight mineralized features, including scutes and surface morphology. Clearing and staining of specimens followed the procedure outlined by Sakata-Haga et al. (2018). Standard length, measured from the tip of the head to the beginning of the tail fin rays, was recorded for each specimen following clearing and staining, and ranged from 10.36 to 21.82 mm. While standard length served as an approximate measure of development, all samples were not raised together, and size did not correspond exactly to degree of scute development.

In total, 19 high-quality, high-resolution images were used to illustrate scute development. Confocal fluorescence images were taken to gather high-detail documentation of bony scutes as mineralized features stained with alizarin red (which emits red fluorescence). All confocal images were composed of 10 µm imaging step sizes through scute depth. Complete images consisted of maximum intensity projection confocal frames stitched together using the Fiji Stitching macro.

2. Mechanical characterization of biomimetic scute assemblies

Study of the development of scutes was combined with mechanical analysis of scute assemblies from different developmental stages to characterize the relationship between scute overlap and bending stiffness. Scute overlap is an important stage in development, as direct interaction of scutes through overlap allows for scutes to behave as an assembly. These interactions may increase the bending stiffness of the system under curvature, as hypothesized. Importantly, natural specimens could not be efficiently and effectively used in mechanical testing due to the small size of specimens during scute development. Adult specimens were also not viable for testing, as scute overlap could not be modified for testing without incurring extensive tissue damage. In place of mechanical tests on natural specimens, confocal images of key scute overlap points informed the fabrication of biomimetic synthetic samples made of silicon and embedded sheet plastic used to mimic skin and scutes.

2.1 Fabrication of biomimetic samples

Three biomimetic samples were fabricated based on particular confocal images. These particular images were selected to best represent key stages of scute overlap: no overlap (Figure 2, based on image #8 in Appendix A), small overlap (Figure 3, based on red fluorescence image), and adult overlap (Figure 4, based on image #19 in Appendix A). Samples will be referred to by these names in the following analysis.

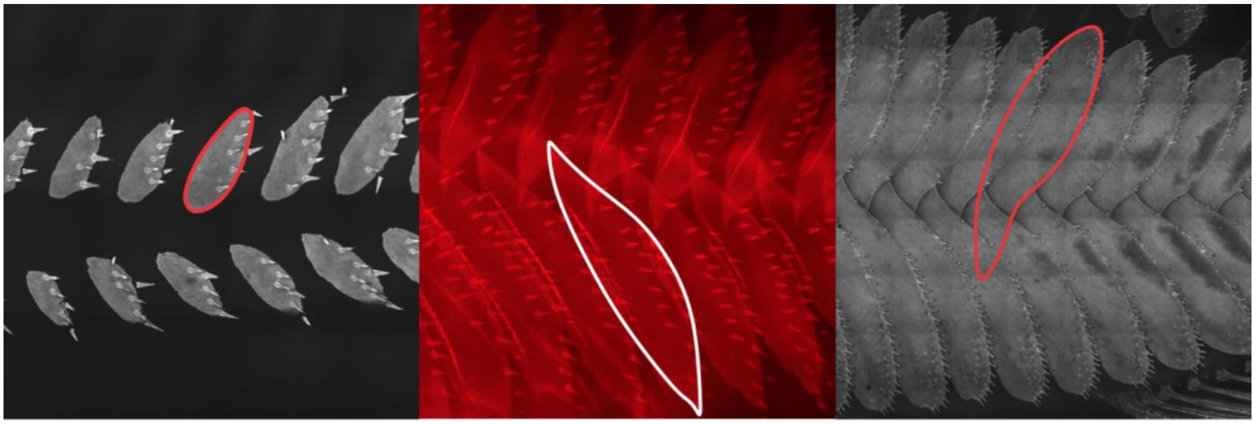

Figure 1. Images of natural scutes overlaid with associated traces of representative scutes. Traces were formed by fitting B-spline curves around the shape natural scutes. Traces were individually laser cut out of delrin to form biomimetic scutes used in synthetic models.

To mimic natural scute shape at these points in development, a B-spline fit was drawn around a standard scute from each selected confocal image (Figure 1). Individual scutes were laser-cut from these traces out of .031-inch-thick delrin, a thin sheet plastic selected to mimic the strength, flexibility, and relative thickness of natural scutes. Synthetic scutes were placed in molds at their respective mimetic degrees of overlap, modeled on representative confocal images. All scutes were placed along an angle of 132°, established from analysis of confocal images. Following placement, scutes were embedded in a casting of 60 grams of Ecoflex 00-30 silicone rubber. Following curing, the Ecoflex substrate for each sample was 0.5 cm thick. Ecoflex 00-30 has commonly been used as a surrogate for biological soft tissues in prior research involving model-making because of its strength, flexibility, and elasticity similar to underlying soft tissues in skin (Sparks et al. 2015; Mori et al. 2016). Here, the relative stiffness and flexibility of delrin scutes compared to that of Ecoflex model the relationship between natural scutes and soft tissue in *C. aeneus*.

After de-molding, samples were trimmed to size 12 cm x 6 cm for testing. This sample length, 12 cm, served as a compromise that enabled the sample with the least scute overlap to support the majority of its own weight during testing, and the sample with the most scute overlap to still experience some flex under its own weight.

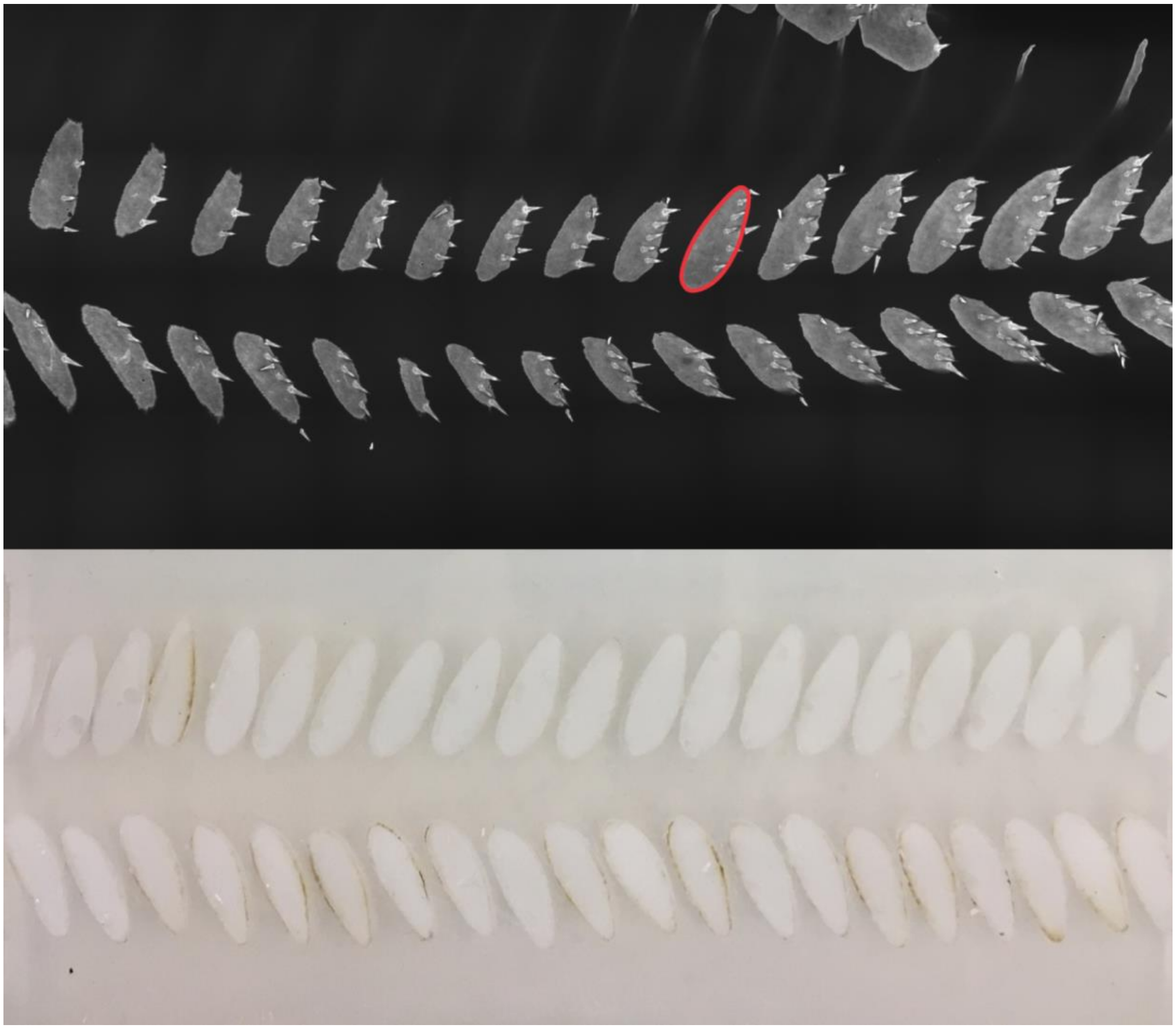

Figure 2. “No overlap” biomimetic sample (bottom) shown below confocal image (top) used as a reference to model this early point in scute development.

Figure 3. “Small overlap” biomimetic sample (right) shown alongside red fluorescence image (left) used as a reference to model this mid-point in scute overlap.

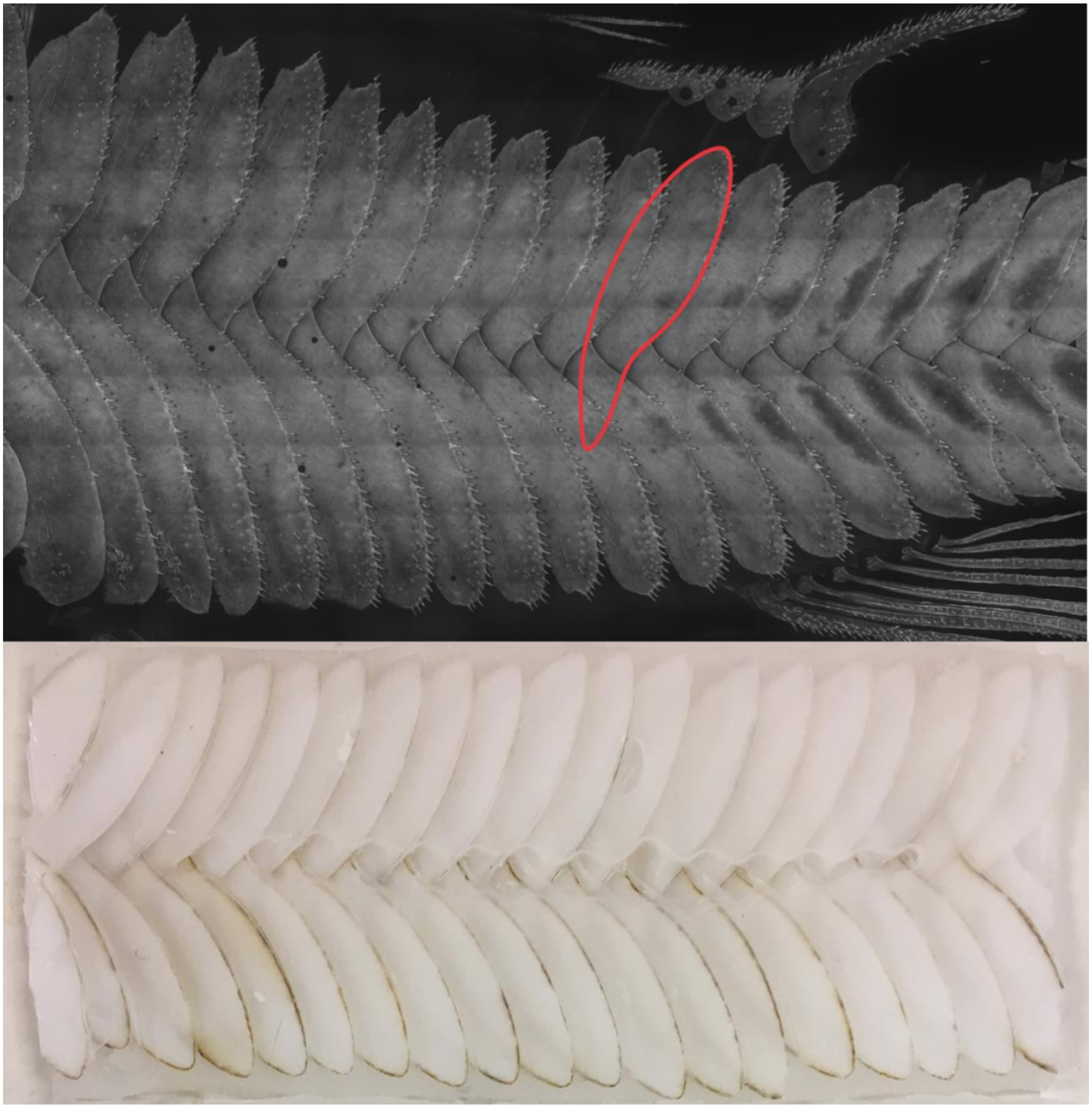

Figure 4. “Adult overlap” biomimetic sample (bottom) shown below confocal image (top) used as a reference to model this degree of scute overlap showcased by fully developed natural specimens.

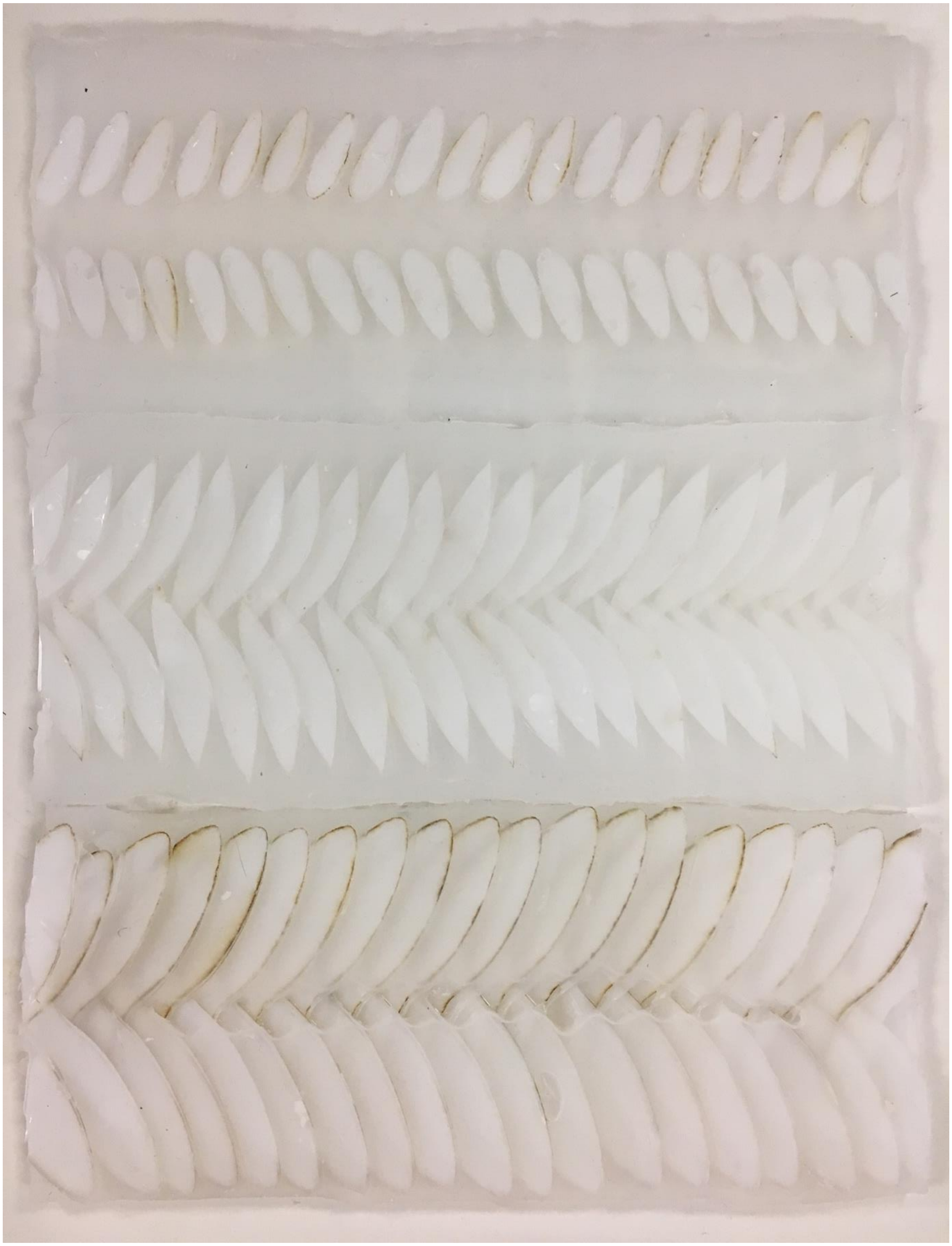

Figure 5. Biomimetic synthetic samples, immediately following de-molding. (Top) No overlap, (middle row) small overlap, and (bottom) adult overlap samples, respectively. All samples were molded to include 21 scutes on each row, to mimic the natural specimens documented in images.

2.2 Analysis of bending stiffness

To compare the flexibility of the three synthetic scute assemblies, bending stiffness (EI) of each sample was calculated using an application of the formula for bending stiffness of a simply supported beam under uniformly-distributed self-weight, ω. This equation and related schematic are shown below as Equation 1. In calculation of these bending stiffnesses, mass for each sample was as follows: 41.66 g (No overlap), 45.04 g (Small overlap), and 46.02 g (Adult overlap). Increase in mass is due to differences in overall scute mass as scutes increase in size.

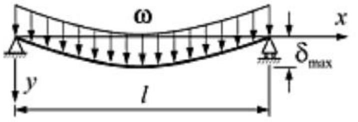

$$y = \frac{\omega x}{24EI}(l^3 - 2l^2 + x^3) \qquad \text{(Eq. 1)}$$

Images were taken of simply supported samples (Figure 6). For each sample, ten point measurements were taken along the midline at relatively evenly spaced distances across the span of the suspended sample. Point measurements were recorded as pixel coordinates using the Fiji image processing software (Schindelin et al. 2012), and scaled as proportions of sample length l. Bending stiffness (EI) of each sample was calculated from the best fit line (y) through these recorded points (Calculations performed in MATLAB R2018b). Results are shown in Table 1. Though this formula is best utilized for small deflections, calculated lines correlate well with the points measured from sample deflections, as shown in Figure 6a.

3. Study of swimming strategy as related to scute development

The pronounced increase in bending stiffness of synthetic scute assemblies as overlap progresses strongly suggests a similar increase in bending stiffness of natural scute assemblies over the course of development. Bending stiffness is inherent to fish functional design, as particular bending stiffness of body regions and fins determines power, propulsion, and ability to maneuver during swimming (Long et al. 2006; Lauder et al. 2011; Cui and Jiang 2016; Jusefi et al. 2017). Previous research of fish swimming, or locomotion, strategies suggests that body stiffness plays a pronounced role in modulating the wave propagation in the undulatory locomotion of many species (Tytell et al. 2010). Simply put, the material stiffness of different regions of a fish's body can either aid or oppose muscle forces to shape the particular wave-like locomotive strategies that propel fishes through the water.

Prior investigation of locomotion as related to bending stiffness suggests that species may be able to compensate for increased stiffness by tuning swimming technique to optimize energetic efficiency (Lauder et al. 2011; Root and Liew 2014; Cui and Jiang 2016; Jusufi et al. 2017). This has been investigated in natural specimens (Hebrank and Hebrank 1986; Long et al. 1996; Nowroozi and Brainerd 2014; Kenaley et al. 2018), swimming robots (Long et al. 2006; Cui and Jiang 2016; Jusufi et al. 2017), and hydrodynamic foils modeled on simplified body shapes of fishes (Lauder et al. 2011; 2012; Shelton et al. 2014; Feilich and Lauder 2015; Lucas et al. 2015). Kinematically, increased stiffness of skin due to scute overlap, as characterized in biomimetic synthetic samples, may result in a functional tradeoff between stiffness and body curvature during normal forward swimming (Tytell et al. 2010; Nowroozi and Brainerd 2014; Root and Liew 2014; Shelton et al. 2014; Lucas et al. 2015; Cui and Jiang 2016; Jusufi et al. 2017). The following analysis will investigate whether larval *C. aeneus* specimens exhibit a decrease in average tail curvature correlated to their degree of scute overlap: no overlap and adult overlap. Operating under the hypothesis that fish scales may serve to contribute to locomotion through energy restitution as somewhat of an "external tendon" (as elaborated on in the Background section), this functional tradeoff between stiffness and curvature may not represent an energetic cost to *C. aeneus*, but merely a balance between protection and flexibility as represented through swimming optimization. Investigating how possible increase in bending stiffness due to scute overlap may influence swimming strategy, specifically average tail curvature, can serve to functionally characterize these important surface features in *C. aeneus*, which could potentially be extended to other members of the Callichthyidae as well as biomimetic models.

3.1 Video analysis of swimming larvae

Analysis of bending stiffness as related to curvature is extended to live specimens through video analysis of the swimming of two different *C. aeneus* larvae groups selected to present extreme ends of scute development: no overlap and adult overlap. These specimen groups are referred to as Group 1 (no overlap) and Group 2 (adult overlap) in the following discussion. Video was captured using a Nikon D5200 DSLR camera, at a frame rate of 25 frames per second (fps). Image resolution and frame rate are not as high as would be afforded with a high-speed image-capture camera, but were sufficient for this exploratory investigation of larval swimming strategies. Groups of larvae were recorded in home tanks over 10-minute, uninterrupted intervals. Subsequent analysis of swimming larvae in each group was based on selections from subsections of this 10-minute video where most forward motion was exhibited by particular specimens.

Video analysis was performed using the Fiji image processing software (Schindelin et al. 2012) paired with curvature analysis in R (R Core Team 2018). The parameter of interest was average tail curvature, specified here as *c*, during normal, forward swimming (i.e. excluding sharp turns or evasion locomotion techniques such as “burst” swimming, as characterized by Budick and O’Malley (2000)). To analyze average tail curvature across groups, splines were manually fit to specimens during forward swimming. Similar spline fitting methodology is outlined by Gazzola et al. (2000) in a study of parameters of larval fish movement. Manual fitting was performed due to low image resolution, but future analyses could script this step to provide more rapid and accurate fits across video frames. Smooth splines were fit using the Fiji Spline Fit macro, and the 100 points making up each spline fit were exported to R (R Core Team 2018) for curvature analysis. In total, 100 manual spline fits for each group were recorded throughout forward swimming from two specimens in each group.

Average tail curvature (c), in mm^{-1}, for each spline fit was calculated in R (R Core Team 2018) as the second derivative of each smooth spline fit, averaged over the tail region. The tail region was specified as the back third of the specimen, according to loose categorization outlined by Gazzola et al. (2000). In general, this tail region exhibited only one direction of curvature, either positive or negative, for each spline recorded, which was important for accurate calculation of average tail curvature.

To compare average tail curvatures across groups, an important assumption was made. Specimens were assumed to be self-similar across groups, meaning that they were roughly the same (including similarity in shape, composition, and density) across developmental stages. Under this assumption, average curvatures (c) can be compared directly through scaling by standard length (L) of the specimens. Average curvatures were scaled by length as Lc, where standard length (L) for Group 1 was 12 mm and standard length for Group 2 was 18.95 mm. Density histograms of calculated average tail curvature for each group are shown in Figure 7.

Average tail curvature during normal forward swimming can be well-described by a Gaussian, or normal, fit. Each density histogram in Figure 7 is overlaid with the related Gaussian fit line calculated from the scaled average curvature data for each group. Notably, some more extreme tail curvatures showcased by specimens in Group 1 are not well-described by a normal distribution, and are left out of the analysis; blue columns of the density histogram for Group 1 are used as representative of the normal range of average tail curvature, and are well-explained by the calculated Gaussian fit. More extreme values are thought to be less characteristic of normal forward swimming strategy, and may represent more pronounced bending during turning or evasion from other larvae, which is not relevant to this preliminary analysis of average tail curvature during forward swimming. Future models could be developed to include these more pronounced curvatures exhibited during evasion or "burst" swimming, as characterized by Budick and O'Malley (2000), in analysis of maximum curvature exhibited by specimens, but this preliminary study focuses on average tail curvature during steady forward swimming, and includes only data points well-described by normal distributions.

As these average curvature values, as scaled by standard length *L*, are well-described with normal distributions, a relevant parameter for comparison of curvature between groups is standard tail curvature for each distribution. Standard tail curvature was calculated as the standard deviation of each group's average tail curvature, and is shown on each plot in Figure 7 as the dashed vertical lines.

Results

1. Qualitative assessment of pattern of scute development

[The full set of microscope images can be found in Appendix A.]

Following documentation of scute development through microscopy, collected images were utilized for qualitative analysis of scute development. As observed in these microscope images, scutes initially appear in the tail region, most specifically in the region of the caudal peduncle, which is the narrowest point of the body directly before the expansion of tail fin rays. As they grow, scutes also overlap first toward the tail region, though scute overlap is generally consistent along the midline of the fish through developmental stages. Interestingly, as scutes grow, some appear to develop independently and then fuse together. Specimens in which scute initiation is complete generally exhibit 21 scutes on the top, or dorsal, row, and 20 scutes on the bottom, or ventral, row. Rows meet at an angle measured to be approximately 132° on one representative image.

2. Bending stiffness of biomimetic scute assemblies

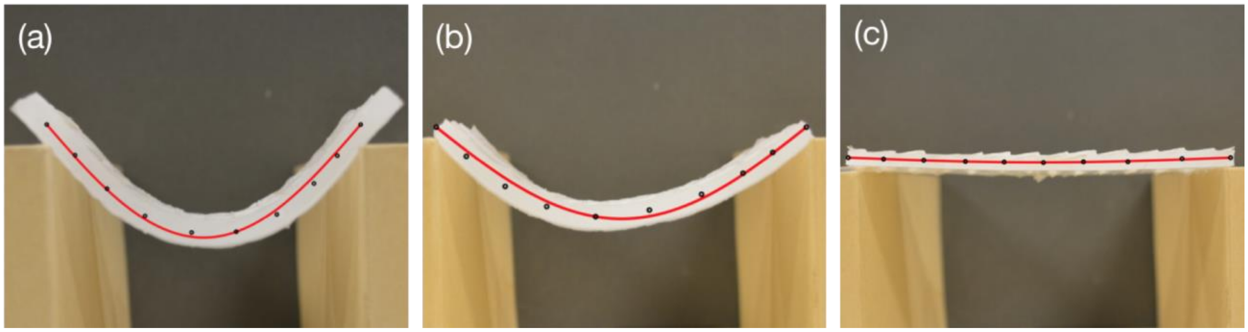

Figure 6. (a) No overlap, (b) small overlap , and (c) adult overlap samples under self-weight for bending analysis. Experimental points measured from images are shown in black, and calculated best-fit lines *y* (Eq. 1) are shown in red. Increase in bending stiffness across samples can be visually noted, as well as quantified in analysis.

Table 1. *Calculated bending stiffness (EI) for each sample*

Sample	Bending stiffness, $EI(\mu N/cm^2)$
No overlap	2124.9746
Small overlap	3346.1108
Adult overlap	69728.2411

Increase of scute size and overlap resulted in pronounced increase of bending stiffness in these synthetic samples. As a baseline, the synthetic scute assembly with no scute overlap bent according to the elastic modulus of the substrate, i.e., Ecoflex 00-30 silicone rubber. Increasing scute overlap increased bending stiffness of the overall system. The slight overlap of medium-sized scales in the small overlap sample resulted in a 57.5% increase in bending stiffness over the sample with no scute overlap. The sample representing adult overlap exhibited a drastic increase of bending stiffness compared to either of the other two samples; bending stiffness increased by 198% relative to the small overlap sample and 318% relative to the no overlap sample. In summary of this analysis, bending stiffness correlated to degree of scute overlap in these synthetic models. This profound increase in bending stiffness, as related to scute overlap in these biomimetic synthetic samples, strongly suggests that bending stiffness of natural scute assemblies also increases as scute overlap increases.

3. Standard tail curvature during swimming as related to degree of scute development

Density histograms of average tail curvatures for specimens exhibiting no scute overlap (Group 1) and adult degree of scute overlap (Group 2) based on video analysis of swimming *C. aeneus* larvae fit Gaussian distributions (see Figure 7 for average tail curvature distributions for each group). In comparing these distributions, groups showcased notable differences in standard tail curvature as related to degree of scute overlap, suggesting that the contribution of scute overlap to overall bending stiffness could influence swimming strategy in *C. aeneus.* Calculated standard curvature of Group 1, specimens showing no scute overlap, was 0.4061, while standard curvature of Group 2, specimens showing adult level of scute overlap, was 0.2115. This nearly 50% lower standard tail curvature during normal forward swimming in specimens with a greater degree of scute overlap suggests that scute overlap may result in a functional tradeoff between curvature and bending stiffness. This finding may indicate functional optimization for energetically efficient swimming and suggests that scute assemblies have a role in locomotion as well as protection in *C. aeneus*.

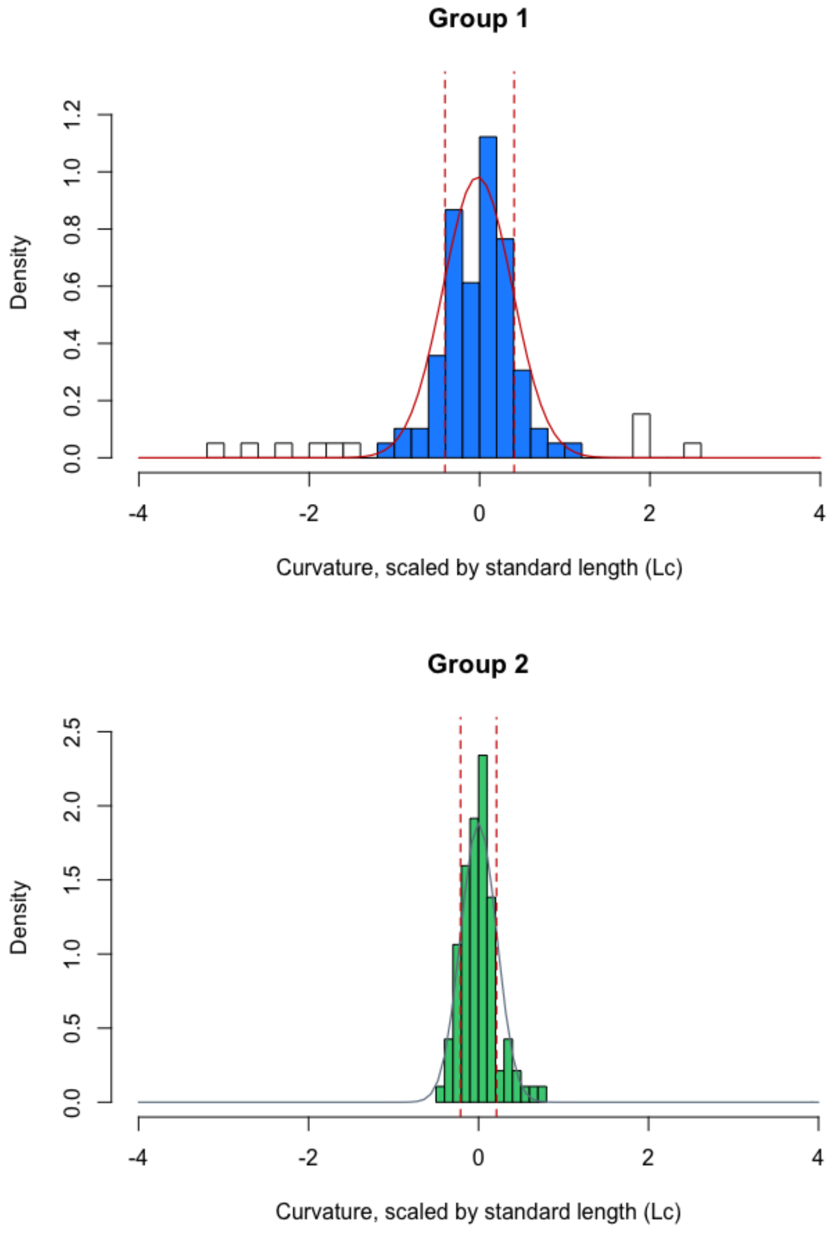

Figure 7. Density histograms of average tail curvatures calculated for each group. Gaussian fits shown as overlaid line, and standard curvature marked on each plot as dashed red lines. Experimental standard curvature for Group 1 is 0.4061, and standard curvature for Group 2 is 0.2115.

Discussion

The present study synthesized developmental and functional insight through investigation of natural *C. aeneus* as well as mechanical analysis of scute overlap in synthetic models. This novel investigation of the scutes of *C. aeneus* contributes to prior mechanical characterization of particular fish scale morphologies (Long et al. 1996; Marino Cugno Garrano et al. 2012; Browning et al. 2013; Zhu et al. 2013; Chintapalli et al. 2014; Vernerey et al. 2014; Vernerey and Barthelat 2014; Funk et al. 2015). Similar to previously-studied scale morphologies (Vernerey and Barthelat 2010; Browning et al. 2013; Ghosh et al. 2014; Szewciw et al. 2017; Kenaley et al. 2018), scute assemblies appear to demonstrate strain-stiffening response due to scute overlap. Additionally, my findings suggest that bending stiffness of scute assemblies may play a role in locomotive strategy of *C. aeneus*, as hypothesized in prior research (Hebrank and Hebrank 1986; Vernerey and Barthelat 2010; Esposito et al. 2012; Feilich and Lauder 2015; Kenaley et al. 2018).

Even though synthetic models of scute assemblies demonstrated a nearly a three-fold increase in bending stiffness correlated to increasing scute overlap, these results cannot be extrapolated to natural specimens without further investigation. Biomimetic synthetic models are fabricated to represent a standard relationship between scute (Sire et al. 2009) and underlying soft tissue density (Sparks et al. 2015). However, specific mechanical characterization of the density of scutes and underlying soft tissues throughout development has yet to be presented for *C. aeneus.* Investigating bending stiffness of naturally-developing scute assemblies is not currently feasible due to the amount of error inherent in mechanical bending tests of small (~ 1 cm standard length) larval specimens. Future research into how to modulate scute development in adult specimens is needed to accurately compare mechanical properties of live specimens to findings from synthetic models.

Quantification of material properties of natural specimens will also contribute to improved understanding of the functional role of natural scutes in locomotive strategy. My preliminary studies made assumptions with respect to how bending stiffness could affect swimming strategy in larval *C. aeneus*. The assumption of self-similarity is likely not biologically accurate. As fish develop and grow, tissues, bones, and other body features develop, which may alter overall material properties beyond just scute development. At this time, little information is available on quantitative changes during development. In order to assess error and accuracy of my preliminary investigation of scute overlap as related to swimming strategy, future characterization of changes in material properties of fishes throughout developmental stages is needed to improve mechanical analyses as related to development.

Conclusions

Overall, this developmental and functional investigation of scutes in a model species, the Bronze Corydoras Catfish (*C. aeneus*), suggests that scute assemblies have not only a protective function, but also a potential role in locomotion as related to increased bending stiffness associated with scute overlap. Fabrication and testing of biomimetic synthetic replicates of scute assemblies revealed a dramatic increase in bending stiffness of scute assemblies following scute overlap, which strongly suggests a similar increase in bending stiffness of natural scute assemblies. Video analysis of live swimming specimens further supported this conclusion by showing that average tail curvature in young *C. aeneus* decreased as predicted for the hypothesized increase in bending stiffness. The findings of this initial analysis of a unique scale structure in a representative species can be extended through further examination of parameters such as surface morphology.

These novel findings can inform future research into scute assemblies as well as the dynamics afforded by unique fish scale morphologies. Extended mechanical study of the unique dermal armor exhibited by *C. aeneus* and related armored catfish can be facilitated with both synthetic models and natural specimens. Future research may build on these findings to develop a more comprehensive understanding of the functions of scute assemblies, and how these unique findings may be translated into innovative designs. Currently, improved understanding of how bending stiffness relates to both protection and efficient locomotion can contribute to the fabrication of unique biomimetic structures based on scute assemblies, such as hybrid armors, efficient swimming structures for aquatic robots, and hydrodynamic foils.

Appendix A: Confocal images

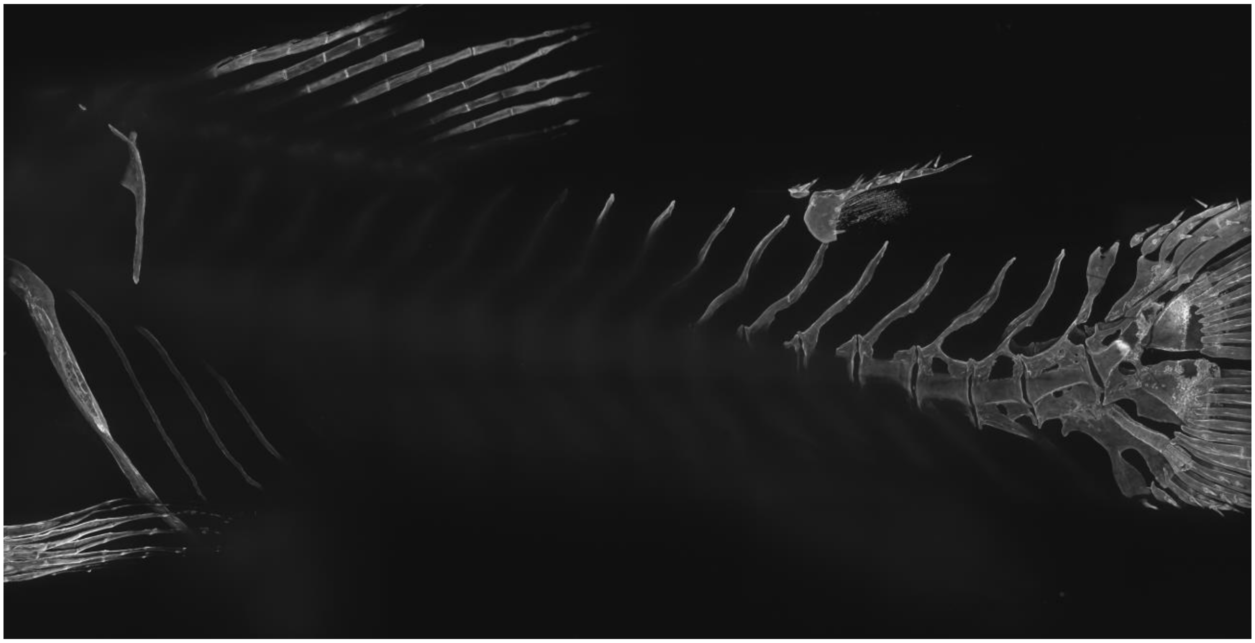

Image 1. 10.36 mm. No scutes.

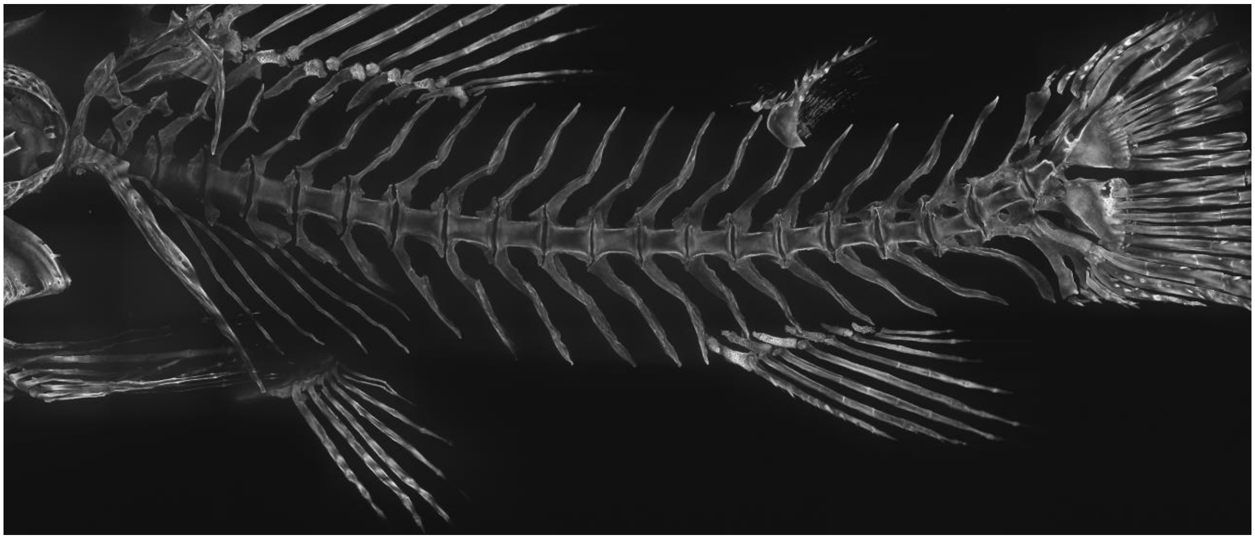

Image 2. 10.59 mm. No scutes.

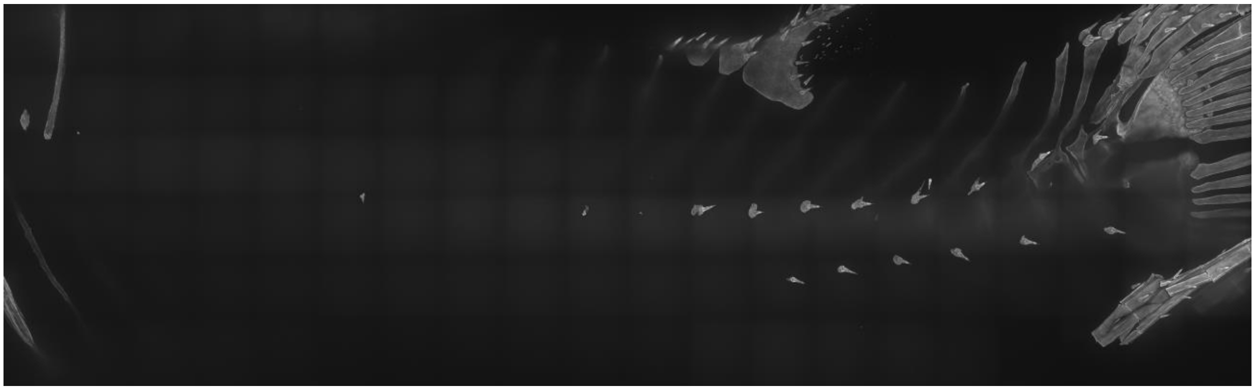

Image 3. 11.07 mm. Tiny scutes are forming toward the tail end of the specimen.

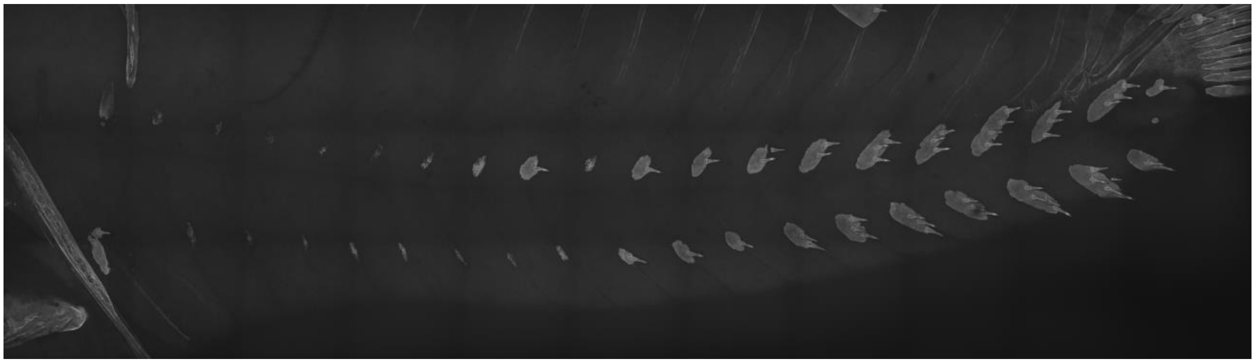

Image 4. 12.30 mm. Scutes have appeared across the full length of the trunk. Scutes are larger in the tail region.

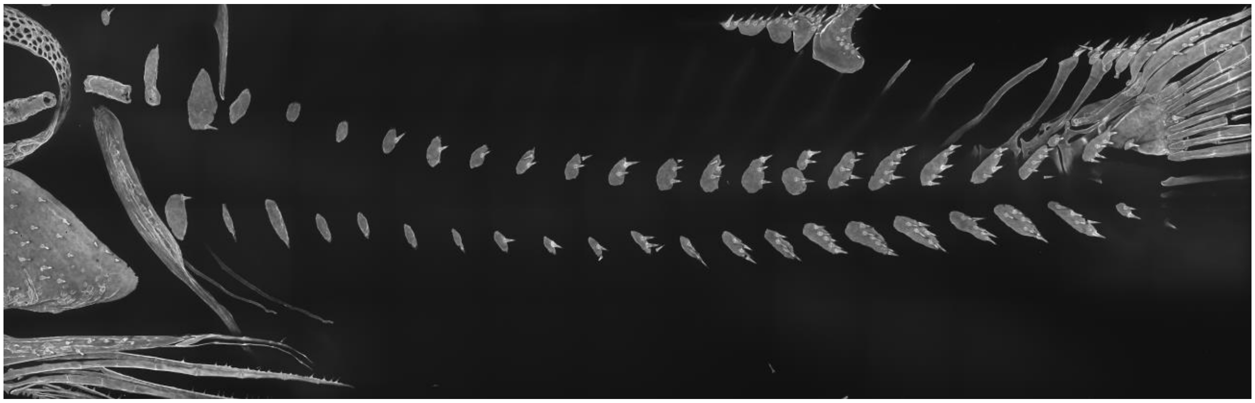

Image 5. 12.34 mm. Scutes progressively grow, with greater growth showcased in the tail half of the specimen. Note two scutes that are developing in two segments (mid top row, and back top row).

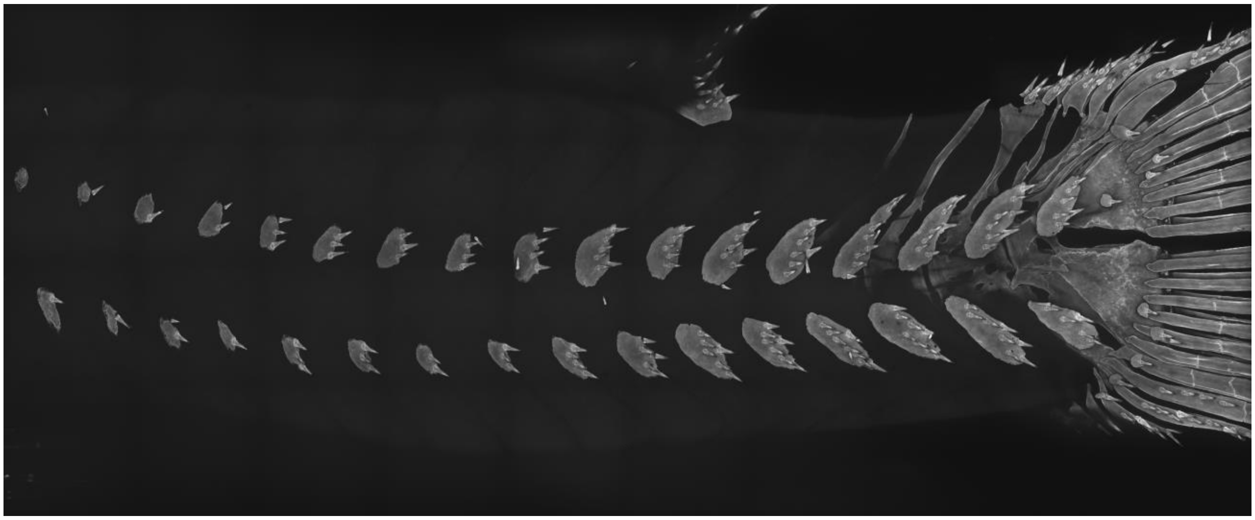

Image 6. 13.01 mm. Small scutes visible along full length of trunk.

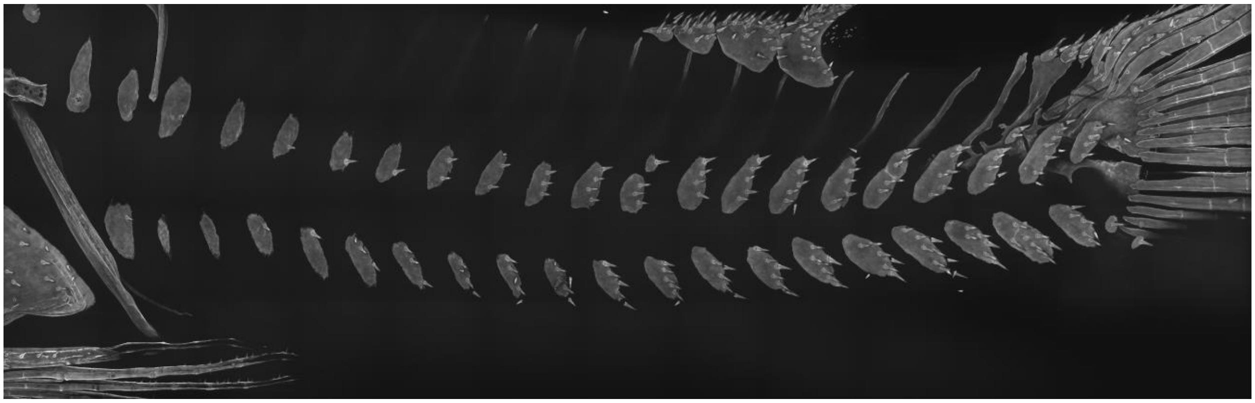

Image 7. 12.89 mm. Two scutes develop in two parts (mid top row, and back top row). One scute (fifth scute from tail, top row), appears to showcase two sections fusing into one scute.

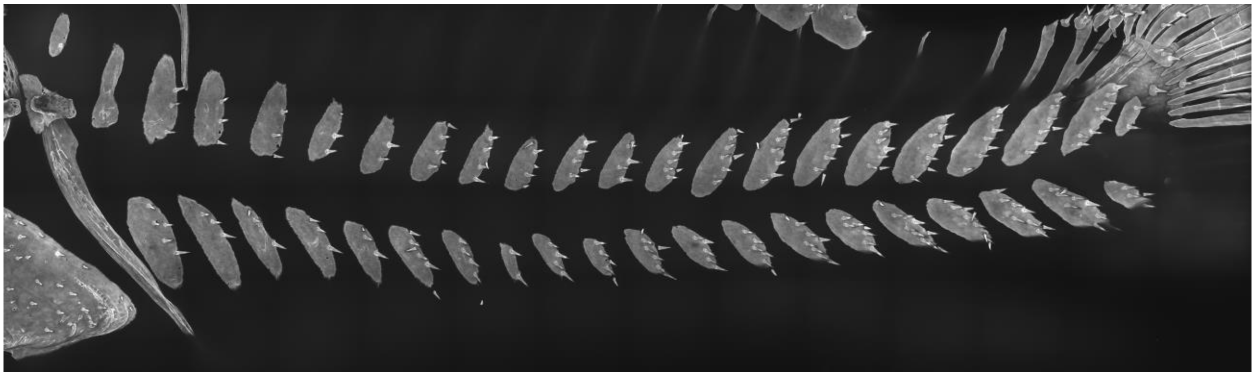

Image 8. 13.95 mm. Scutes in middle region appear smallest, and scutes in tail region appear largest, generally.

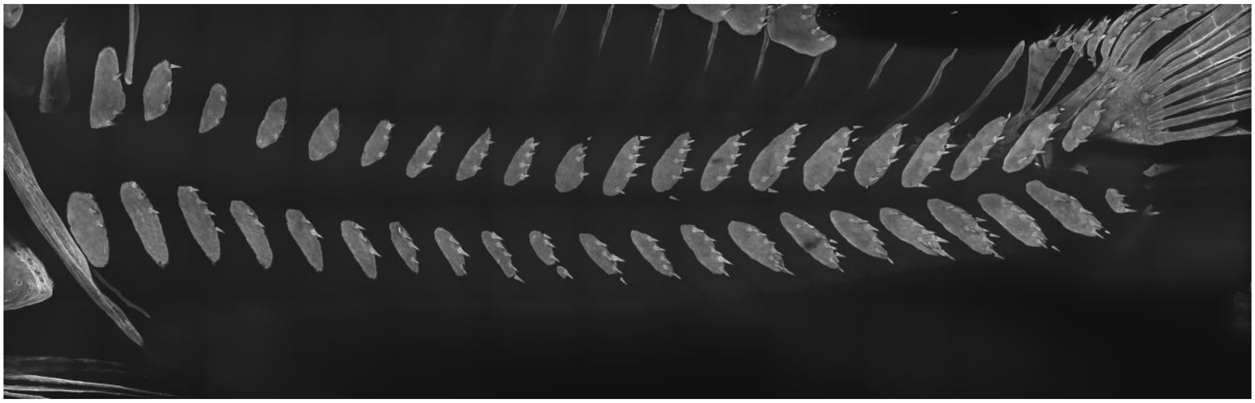
Image 9. 13.35 mm. One scute (mid bottom row) appears to develop in two pieces.

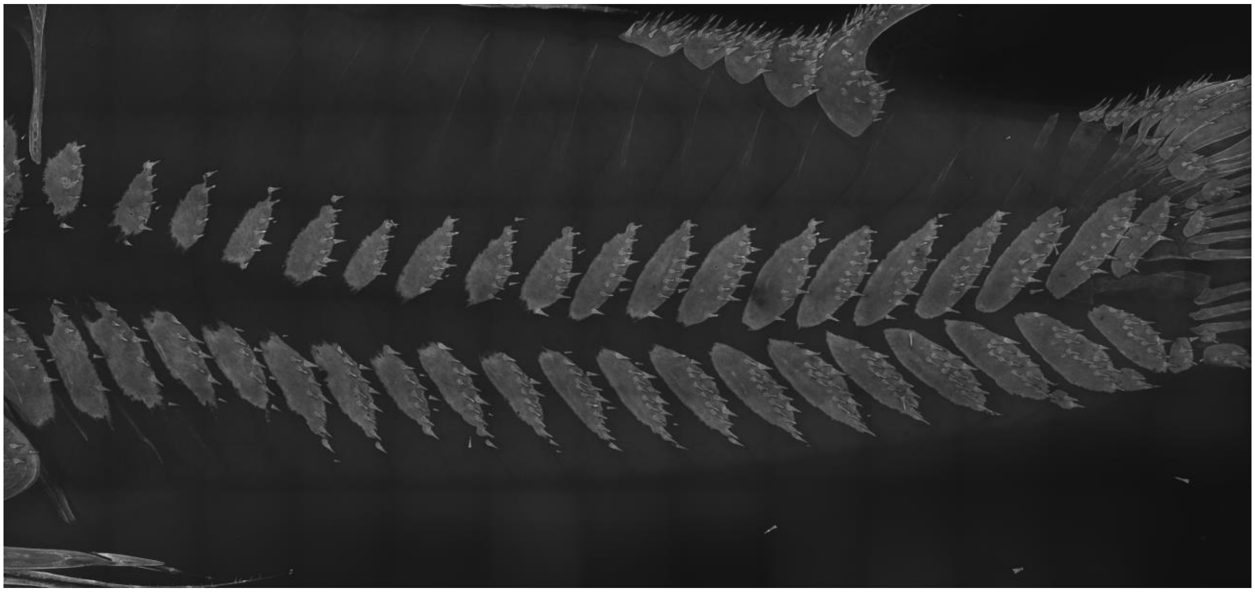
Image 10. 15.48 mm. Scutes are nearing overlap in the tail third of the specimen.

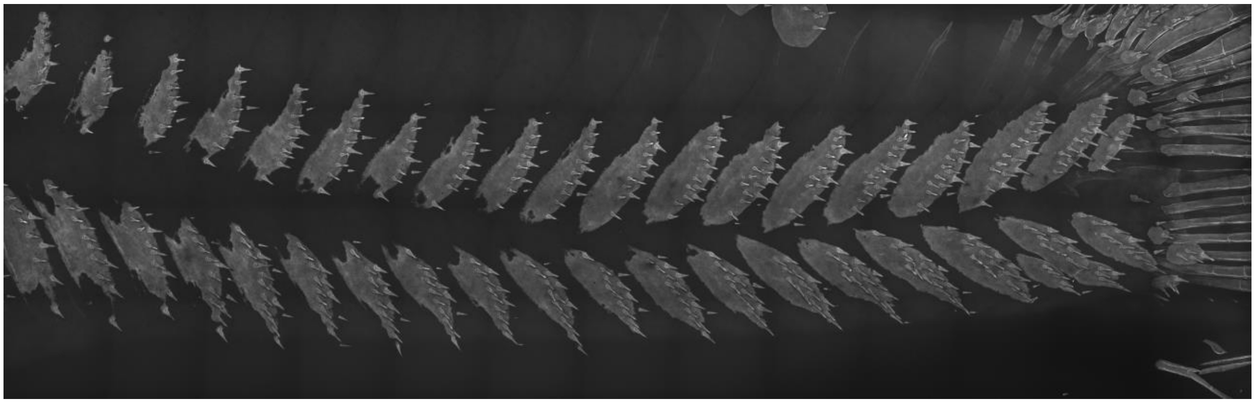
Image 11. 16.14 mm. Black regions of front scutes may be imaging artifacts.

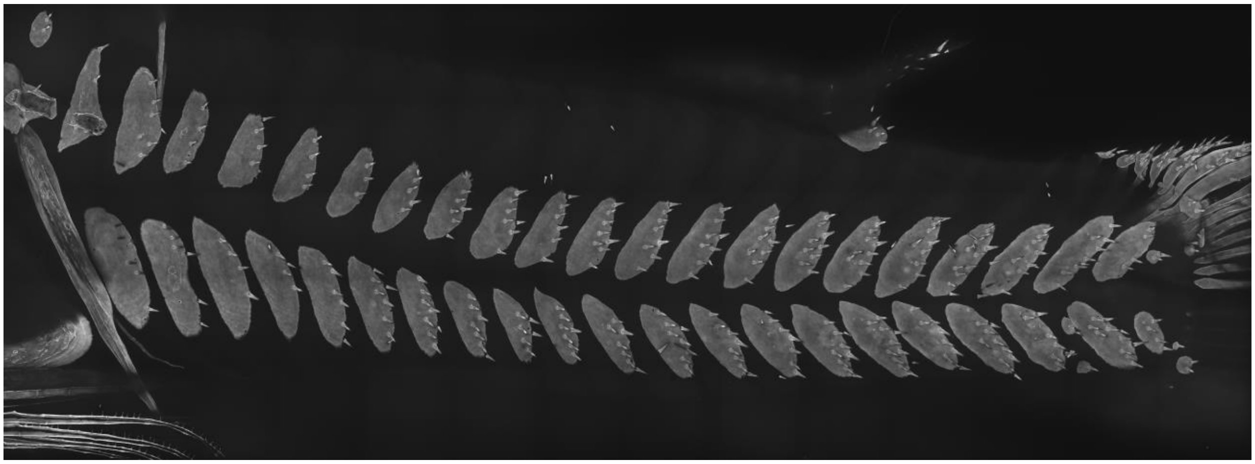

Image 12. 17.3 mm.

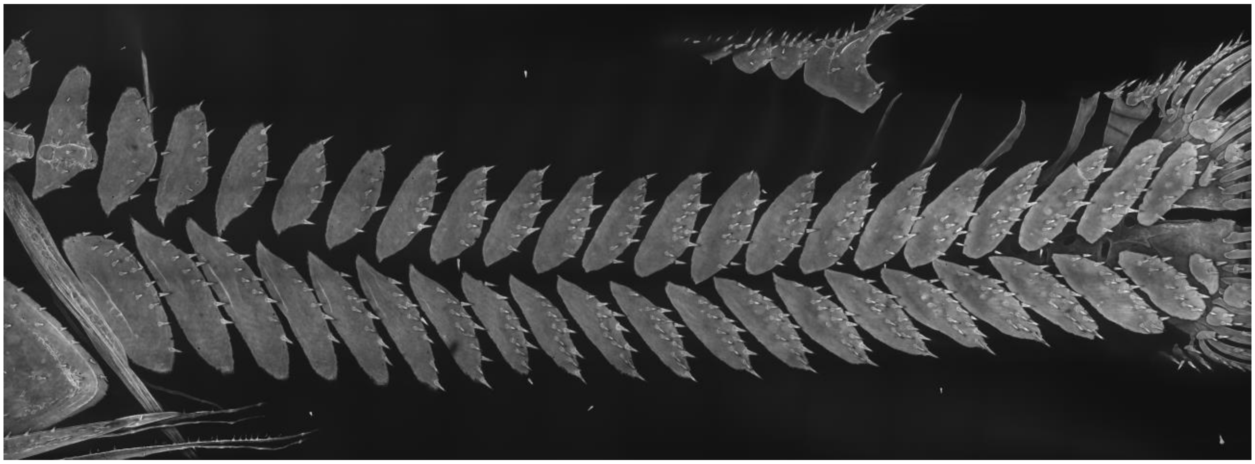

Image 13. 15.1 mm. Scutes in tail region and one scute pair toward the head are very close to overlapping.

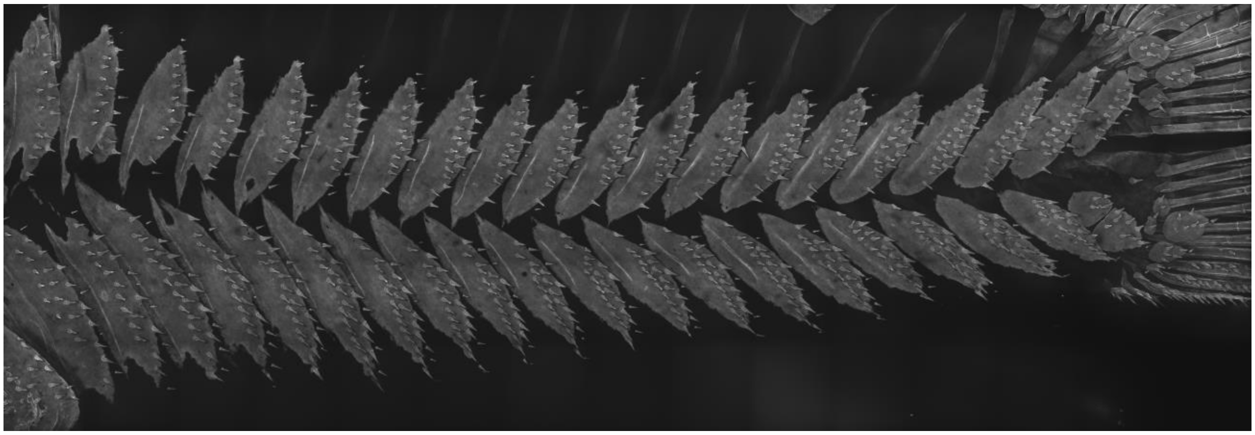

Image 14. 17.3 mm. In this specimen, scutes toward the head appear largest in length. Scutes are beginning to overlap in their rows.

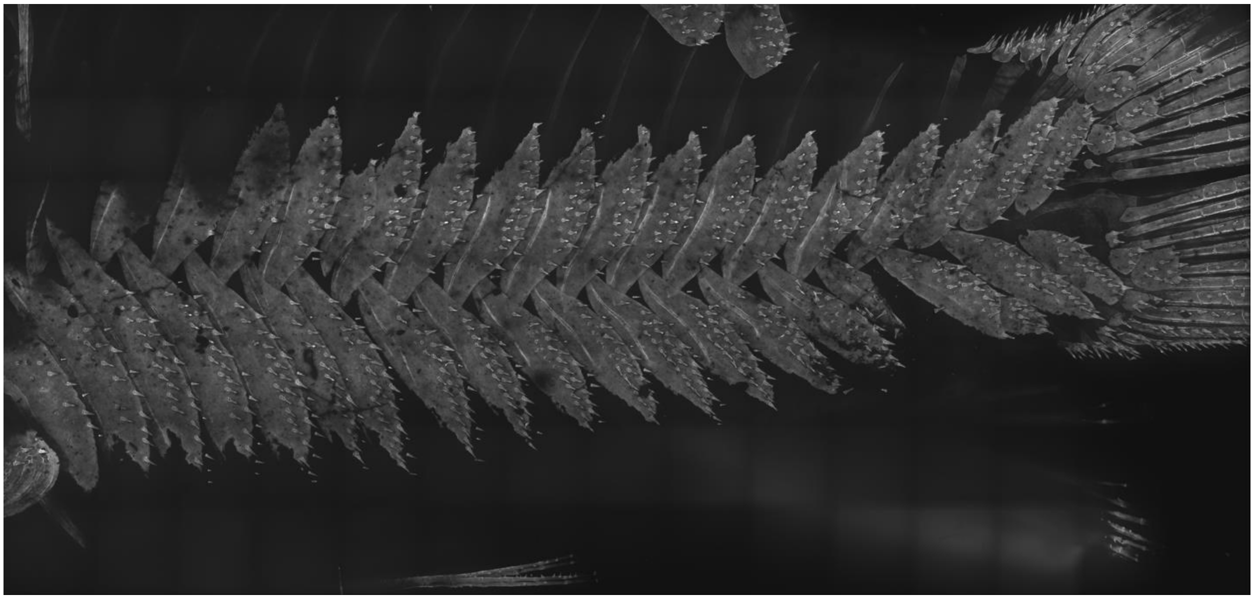

Image 15. 14.53 mm. Some scutes are broken.

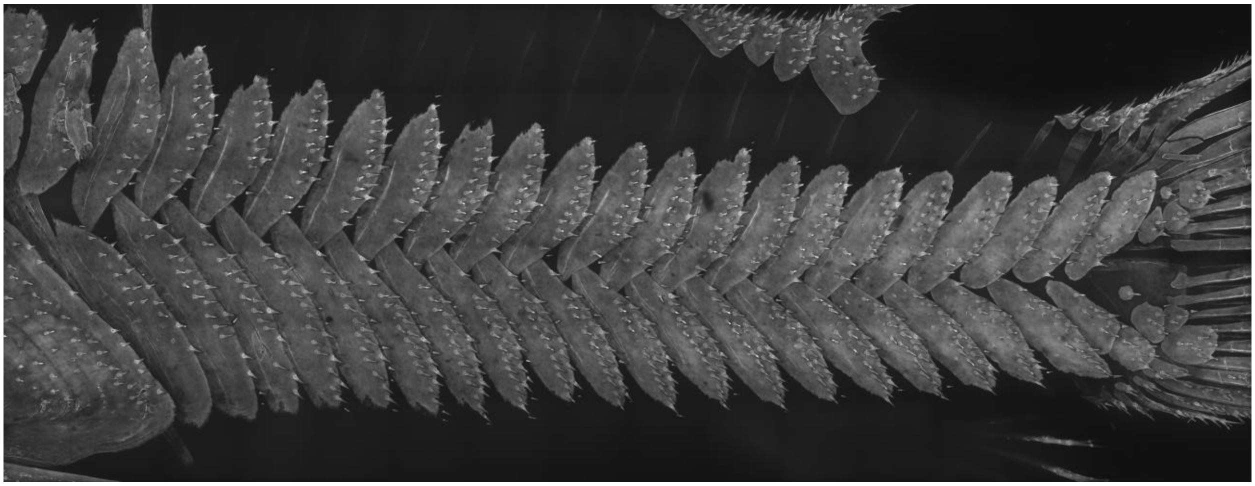

Image 16. 16.79 mm. Scales in rows begin to overlap. Overlap between rows is staggered, as clearly showcased toward the head.

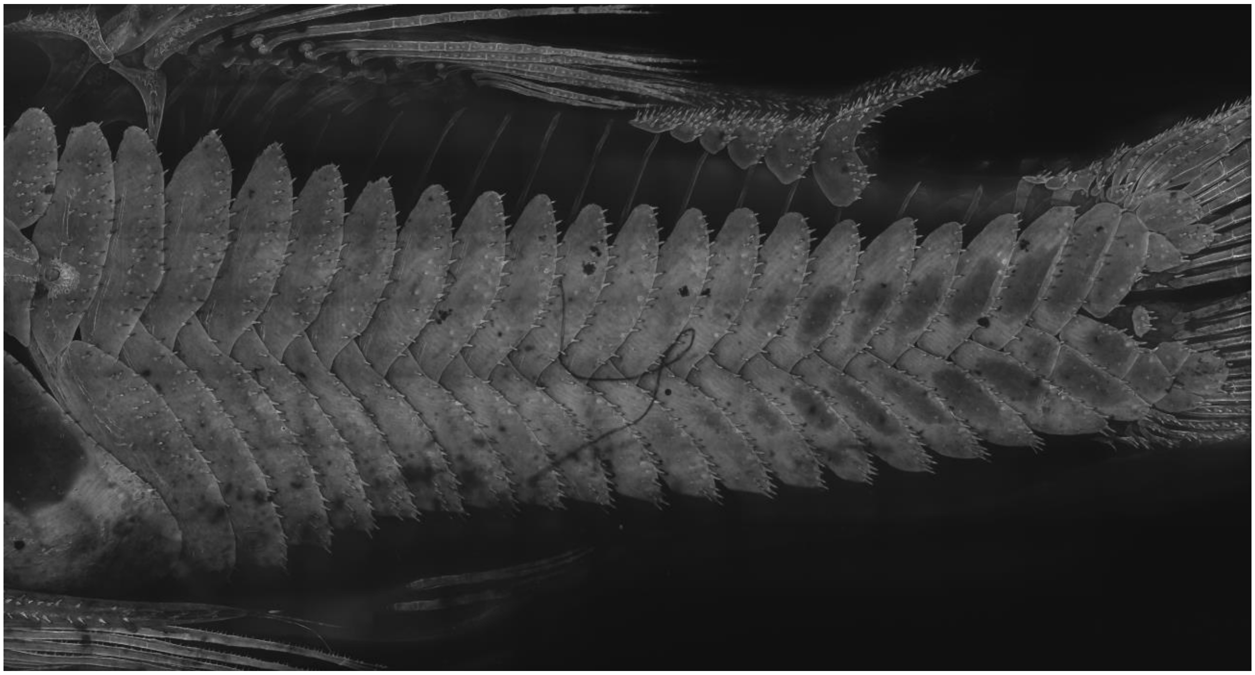

Image 17. 17.36 mm. Scutes showcase overlap across full length of trunk. Small line is a hair caught on specimen during imaging.

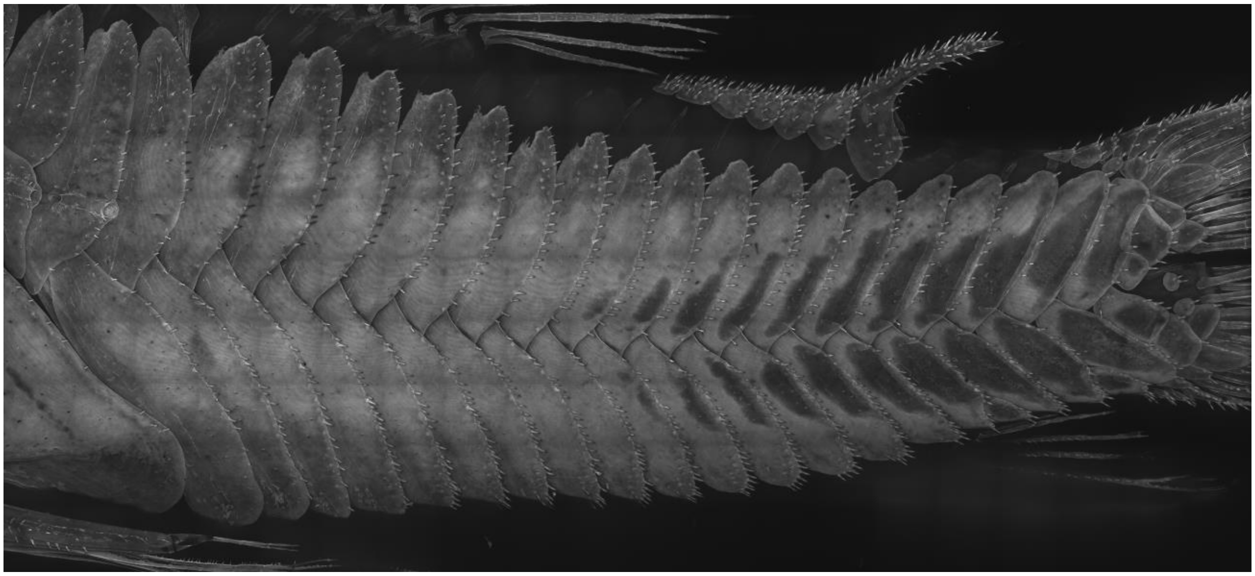

Image 18. 20.29 mm. Scutes showcase an adult level of overlap. Scutes at extreme end of tail region are segmented.

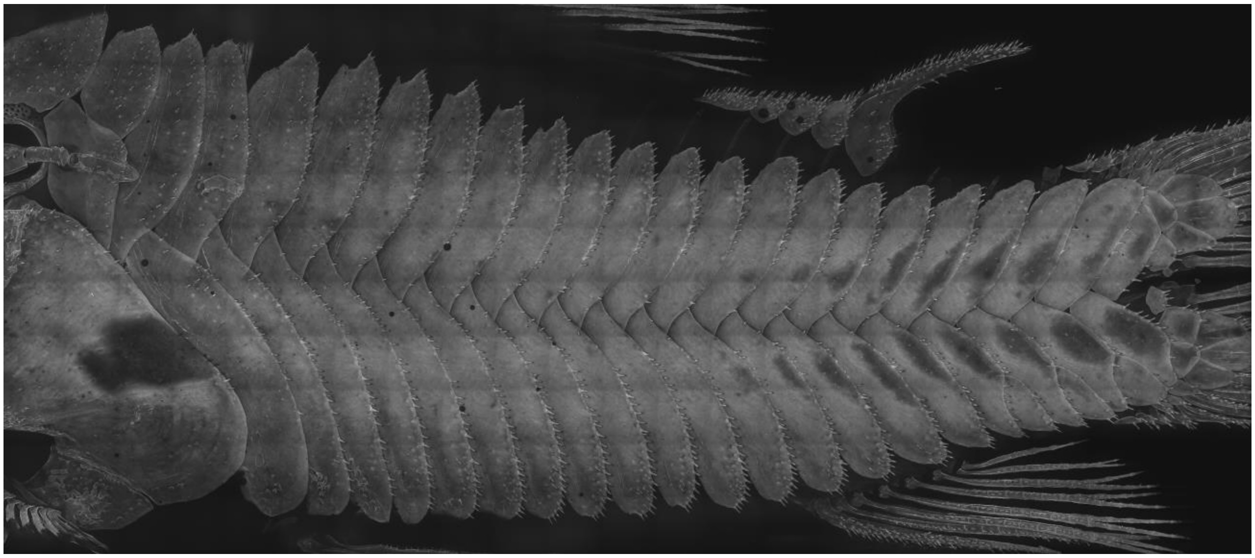

Image 19. 20.40 mm. Scutes showcase an adult level of overlap. Small black dots are imaging artifacts.

References

Blake RW. 2004. Fish functional design and swimming performance. Journal of Fish Biology. 65(5):1193–1222. doi:10.1111/j.0022-1112.2004.00568.x.

Bräger Z, Staszny Á, Mertzen M, Moritz T, Horváth G. 2017. Fish scale Identification: from individual to species-specific shape variability. Acta Ichthyologica et Piscatoria; Szczecin. 47(4):331–338. doi:http://dx.doi.org.colorado.idm.oclc.org/10.3750/AIEP/02245.

Browning A, Ortiz C, Boyce MC. 2013. Mechanics of composite elasmoid fish scale assemblies and their bioinspired analogues. Journal of the Mechanical Behavior of Biomedical Materials. 19:75–86. doi:10.1016/j.jmbbm.2012.11.003.

Budick SA, O'Malley DM. 2000a. Locomotor repertoire of the larval zebrafish: swimming, turning and prey capture. Journal of Experimental Biology. 203(17):2565–2579.

Chen P-Y, Schirer J, Simpson A, Nay R, Lin Y-S, Yang W, Lopez MI, Li J, Olevsky EA, Meyers MA. 2011. Predation versus protection: fish teeth and scales evaluated by nanoindentation. Journal of Materials Research; Warrendale. 27(1):100–112. doi:http://dx.doi.org.colorado.idm.oclc.org/10.1557/jmr.2011.332.

Chintapalli RK, Mirkhalaf M, Dastjerdi AK, Barthelat F. 2014. Fabrication, testing and modeling of a new flexible armor inspired from natural fish scales and osteoderms. Bioinspiration & Biomimetics. 9(3):036005. doi:10.1088/1748-3182/9/3/036005.

Cui Z, Jiang H. 2016. Design, analysis, and simulation of a planar serial–parallel mechanism for a compliant robotic fish with variable stiffness. Advances in Mechanical Engineering. 8(8):1687814016660927. doi:10.1177/1687814016660927.

Elliot, DG. 2000. Integumentary system. In: Ostrander GK, editor. The Laboratory Fish. San Francisco: Academic Press. p. 95-108.

Esposito CJ, Tangorra JL, Flammang BE, Lauder GV. 2012. A robotic fish caudal fin: effects of stiffness and motor program on locomotor performance. Journal of Experimental Biology. 215(1):56–67. doi:10.1242/jeb.062711.

Feilich KL, Lauder GV. 2015. Passive mechanical models of fish caudal fins: effects of shape and stiffness on self-propulsion. Bioinspiration & Biomimetics.10(3):036002. doi:10.1088/1748-3190/10/3/036002.

Funk N, Vera M, Szewciw LJ, Barthelat F, Stoykovich MP, Vernerey FJ. 2015. Bioinspired fabrication and characterization of a synthetic fish skin for the protection of soft materials. ACS Applied Materials & Interfaces. 7(10):5972–5983. doi:10.1021/acsami.5b00258.

Gazzola M, Argentina M, Mahadevan L. 2014. Scaling macroscopic aquatic locomotion. Nature Physics. 10(10):758–761. doi:10.1038/nphys3078.

Grande L. 2010. An empirical synthetic pattern study of gars (Lepisosteiformes) and closely related species, based mostly on skeletal anatomy. The resurrection of Holostei. American Society of Ichthyologists and Herpetologists Special Publication 6.

Harder W. 1976. Anatomy of fishes. Sokoloff T: S, editor. Stuttgart, Germany: Schweizerbart Science Publishers.

Hebrank MR. 1980. Mechanical properties and locomotor functions of eel skin. Biological Bulletin. 158(1):58–68. doi:10.2307/1540758.

Hebrank MR, Hebrank JH. 1986. The mechanics of fish skin: lack of an "external tendon" role in two teleosts. Biological Bulletin. 171(1):236–247. doi:10.2307/1541920.

Ibañez A, Jawad L, Sadighzadeh Z. 2016. Morphometric variation of fish scales among some species of the family Lutjanidae from Iranian waters. Cahiers de Biologie Marine. 57:289–295.

Ibañez AL, Cowx IG, O'higgins P. 2009. Variation in elasmoid fish scale patterns is informative with regard to taxon and swimming mode. Zoological Journal of the Linnean Society. 155(4):834–844. doi:10.1111/j.1096-3642.2008.00465.x.

Jawad L. 2005. Comparative morphology of scales of four teleost fishes from Sudan and Yemen. Journal of Natural History. 39:2643–2660. doi:10.1080/00222930500102801.

Jusufi A, Vogt DM, Wood RJ, Lauder GV. 2017. Undulatory swimming performance and body stiffness modulation in a soft robotic fish-inspired physical model. Soft Robotics. 4(3):202–210. doi:10.1089/soro.2016.0053.

Kenaley CP, Sanin A, Ackerman J, Yoo J, Alberts A. 2018. Skin stiffness in ray-finned fishes: contrasting material properties between species and body regions. Journal of Morphology. 279(10):1419–1430. doi:10.1002/jmor.20877.

Lauder GV, Flammang B, Alben S. 2012. Passive robotic models of propulsion by the bodies and caudal fins of fish. Integrative and Comparative Biology. 52(5):576–587. doi:10.1093/icb/ics096.

Lauder GV, Madden PGA, Tangorra JL, Anderson E, Baker TV. 2011. Bioinspiration from fish for smart material design and function. Smart Materials and Structures. 20(9):094014. doi:10.1088/0964-1726/20/9/094014.

Long J, Hale M, Mchenry M, Westneat M. 1996. Functions of fish skin: flexural stiffness and steady swimming of longnose gar, *Lepisosteus osseus*. Journal of Experimental Biology. 199(10):2139–2151.

Long JH, Koob TJ, Irving K, Combie K, Engel V, Livingston N, Lammert A, Schumacher J. 2006. Biomimetic evolutionary analysis: testing the adaptive value of vertebrate tail stiffness in autonomous swimming robots. Journal of Experimental Biology. 209(23):4732–4746. doi:10.1242/jeb.02559.

Lucas KN, Thornycroft PJM, Gemmell BJ, Colin SP, Costello JH, Lauder GV. 2015. Effects of non-uniform stiffness on the swimming performance of a passively-flexing, fish-like foil model. Bioinspiration & Biomimetics. 10(5):056019. doi:10.1088/1748-3190/10/5/056019.

Marino Cugno Garrano A, La Rosa G, Zhang D, Niu L-N, Tay FR, Majd H, Arola D. 2012. On the mechanical behavior of scales from *Cyprinus carpio*. Journal of the Mechanical Behavior of Biomedical Materials. 7:17–29. doi:10.1016/j.jmbbm.2011.07.017.

Mori N, Morimoto Y, Takeuchi S. 2016. Stretchable culture device of skin-equivalent with improved epidermis thickness. In: 2016 IEEE 29th International Conference on Micro Electro Mechanical Systems (MEMS). p. 259–262.

Nelson JS, Grande TC, Wilson MVH. 2016. Fishes of the world, 5th Edition. New Jersey: Wiley.

Nowroozi BN, Brainerd EL. 2014. Importance of mechanics and kinematics in determining the stiffness contribution of the vertebral column during body-caudal-fin swimming in fishes. Zoology. 117(1):28–35. doi:10.1016/j.zool.2013.10.003.

R Core Team. 2018. R: A language and environment for statistical computing. R Foundation for Statistical Computing, Vienna, Austria. URL https://www.R-project.org/.

Rivera-Rivera CJ., Montoya-Burgos JI. 2017. Trunk dental tissue evolved independently from underlying dermal bony plates but is associated with surface bones in living odontode-bearing catfish. Proceedings of the Royal Society B: Biological Sciences. 284(1865):20171831. doi:10.1098/rspb.2017.1831.

Root RG, Liew CW. 2014. Computational and mathematical modeling of the effects of tailbeat frequency and flexural stiffness in swimming fish. Zoology. 117(1):81–85. doi:10.1016/j.zool.2013.11.003.

Rudykh S, Boyce MC. 2014. Analysis of elasmoid fish imbricated layered scale-tissue systems and their bio-inspired analogues at finite strains and bending. IMA Journal of Applied Mathematics. 79(5):830–847. doi:10.1093/imamat/hxu005.

Sakata-Haga H, Uchishiba M, Shimada H, Tsukada T, Mitani M, Arikawa T, Shoji H, Hatta T. 2018. A rapid and nondestructive protocol for whole-mount bone staining of small fish and Xenopus. Scientific Reports (Nature Publisher Group); London. 8:1–7. doi:http://dx.doi.org.colorado.idm.oclc.org/10.1038/s41598-018-25836-4.

Schindelin J, Arganda-Carreras I, Frise E, Kaynig V, Longair M, Pietzsch T, Preibisch S, Rueden C, Saalfeld S, Schmid B, et al. 2012. Fiji: an open-source platform for biological-image analysis. Nature Methods. 9(7):676–682. doi:10.1038/nmeth.2019.

Schultze HP. 2018. Hard tissues in fish evolution: history and current issues. Société Française d’Ichtyologie. 42(1):29–39. doi:10.26028/cybium/2018-421-003.

Shelton RM, Thornycroft PJM, Lauder GV. 2014. Undulatory locomotion of flexible foils as biomimetic models for understanding fish propulsion. Journal of Experimental Biology. 217(12):2110–2120. doi:10.1242/jeb.098046.

Sire J-Y. 1993. Development and fine structure of the bony scutes in *Corydoras arcuatus* (Siluriformes, callichthyidae). Journal of Morphology. 215(3):225–244. doi:10.1002/jmor.1052150305.

Sire J-Y, Akimenko M-A. 2004. Scale development in fish: a review, with description of sonic hedgehog (shh) expression in the zebrafish (*Danio rerio*). The International Journal of Developmental Biology. 48(2–3):233–247. doi:10.1387/ijdb.031767js.

Smolyar IV, Bromage TG. 2004. Discrete model of fish scale incremental pattern: a formalization of the 2D anisotropic structure. ICES Journal of Marine Science. 61(6):992–1003. doi:10.1016/j.icesjms.2004.07.013.

Sparks JL, Vavalle NA, Kasting KE, Long B, Tanaka ML, Sanger PA, Schnell K, Conner-Kerr TA. 2015. Use of silicone materials to simulate tissue biomechanics as related to deep tissue injury. Advances in Skin & Wound Care. 28(2):59–68. doi:10.1097/01.ASW.0000460127.47415.6e.

Szewciw L, Barthelat F. 2017. Mechanical properties of striped bass fish skin: evidence of an exotendon function of the stratum compactum. Journal of the Mechanical Behavior of Biomedical Materials. 73:28–37. doi:10.1016/j.jmbbm.2016.09.031.

Szewciw L, Zhu D, Barthelat F. 2017. The nonlinear flexural response of a whole teleost fish: contribution of scales and skin. Journal of the Mechanical Behavior of Biomedical Materials. 76:97–103. doi:10.1016/j.jmbbm.2017.06.014.

Szypula J. 2005. Scale radius growth versus standard length growth in some fish species. Archives of Polish Fisheries; Olsztyn. 13(2):235–249.

Torres FG, Malásquez M, Troncoso OP. 2015. Impact and fracture analysis of fish scales from *Arapaima gigas*. Materials Science and Engineering: C. 51:153–157. doi:10.1016/j.msec.2015.02.034.

Tytell ED, Borazjani I, Sotiropoulos F, Baker TV, Anderson EJ, Lauder GV. 2010. Disentangling the functional roles of morphology and motion in the swimming of fish. Integrative and Comparative Biology. 50(6):1140–1154.

Vernerey FJ, Barthelat F. 2010. On the mechanics of fishscale structures. International Journal of Solids and Structures. 47(17):2268–2275. doi:10.1016/j.ijsolstr.2010.04.018.

Vernerey FJ, Barthelat F. 2014. Skin and scales of teleost fish: simple structure but high performance and multiple functions. Journal of the Mechanics and Physics of Solids. 68:66–76. doi:10.1016/j.jmps.2014.01.005.

Vernerey FJ, Musiket K, Barthelat F. 2014. Mechanics of fish skin: a computational approach for bio-inspired flexible composites. International Journal of Solids and Structures. 51(1):274–283. doi:10.1016/j.ijsolstr.2013.10.001.

Wainwright SA, Vosburgh F, Hebrank JH. 1978. Shark skin: function in locomotion. Science. 202(4369):747. doi:10.1126/science.202.4369.747.

White ZW, Vernerey FJ. 2018. Armours for soft bodies: how far can bioinspiration take us? Bioinspiration & Biomimetics. 13(4):041004. doi:10.1088/1748-3190/aababa.

Whitear, M. 1986. Dermis. In: Bereiter-Hahn J, Matolsky AG, Richards KS, editors. Biology of the Integument 2: Vertebrates. Berlin: Springer-Verlag. p. 39-64.

Zhu D, Ortega CF, Motamedi R, Szewciw L, Vernerey F, Barthelat FJ. 2012. Structure and mechanical performance of a “modern” fish scale. Advanced Engineering Materials. 14(4):B185–B194. doi:10.1002/adem.201180057.

Zhu D, Szewciw L, Vernerey FJ, Barthelat F. 2013. Puncture resistance of the scaled skin from striped bass: collective mechanisms and inspiration for new flexible armor designs. Journal of the Mechanical Behavior of Biomedical Materials. 24:30–40. doi:10.1016/j.jmbbm.2013.04.011.